Applied Energy 223 (2018) 229–248

Contents lists available at ScienceDirect

Applied Energy

journal homepage: www.elsevier.com/locate/apenergy

# Economic assessment of photovoltaic battery systems based on household load profiles

S. Schopfer[a,*], V. Tiefenbeck[a], T. Staake[b]

[a] Chair of Information Management, Department of Management, Technology and Economics, ETH Zurich, Weinbergstrasse 58 (WEV G), CH-8092 Zurich, Switzerland
[b] Energy Efficient Systems Group, Department of Information Systems and Applied Computer Sciences, University of Bamberg, An der Weberei 5, 96047 Bamberg, Germany

## HIGHLIGHTS

- Techno-economic model analyzing profitability of PV-battery systems.
- Heterogeneity analysis based on 4190 real-world load profiles.
- Predictor for optimal PV-battery system configuration for individual households.
- Large variance in profitability, even for households with comparable annual demand.
- Good prediction accuracy with only one month of smart-meter data.

## ARTICLE INFO

*Keywords:*
Solar energy
Storage
Smart-meter data
Techno-economic simulation
Load profile
Machine learning

## ABSTRACT

Technical advances and decreasing costs of photovoltaic (PV) and battery (B) systems are key drivers for the consumer-prosumer transition in many countries. However, the installation of a photovoltaic-battery (PVB) system is not equally profitable for all consumers. This study systematically assesses how heterogeneity in real-world electricity load profiles affects the optimal system configuration and profitability of PVB systems. To that end, we develop a techno-economic simulation model that optimizes the PVB configuration for given electricity load profiles. The analysis uses real-world energy consumption data from 4190 households and is conducted for current electricity rates and weather conditions in Zurich, Switzerland. To account for future price reductions of PV and PVB systems, we conduct a sensitivity analysis that assesses how different cost scenarios influence optimal system configuration and profitability. Finally, we develop and validate a machine learning algorithm that can predict system profitability based only on a limited set of features and on shorter measurement timeframes of smart-meter data. We find that under the current cost scenario (PV: 2000 €/kWp, B: 1000 €/kWh) and without subsidies, about 40% of the analyzed households reach a positive net present value (NPV) for a PV-system, but only for 0.1% of households is the integration of a battery profitable. Under the most optimistic cost scenario for both technologies (PV: 1000 €/kWp, B: 250 €/kWh), 99.9% of the households benefit from the integration of battery storage into their optimal system configuration, with a mean installed PV power of 4.4 kWp and a mean battery size of 9.6 kWh. In all cost scenarios, system profitability varies considerably between households, even for households with comparable total annual demand, primarily due to the heterogeneity in the load profiles. Thus, being able to identify households for whom the installation is profitable is important. The proposed machine learning algorithm predicts optimal configuration, profitability, self-sufficiency, and self-sufficiency ratios with good accuracy, even when only relatively short timeframes of smart-meter data are available. The results of this study are relevant for households making individual investment decisions as well as for utility companies to more effectively identify and approach relevant customers for the installation of PVB systems. Furthermore, the findings enable policymakers to determine the critical levers for increasing private investments into PVB systems in their region and to predict how future developments like component costs will affect the future diffusion of these systems.

* Corresponding author.
*E-mail address:* sandro.schopfer@ethz.ch (S. Schopfer).

https://doi.org/10.1016/j.apenergy.2018.03.185
Received 25 November 2017; Received in revised form 29 March 2018; Accepted 30 March 2018
Available online 27 April 2018

**Nomenclature**

*Abbreviations*

| | |
|---|---|
| B | battery |
| DoD | depth of discharge (–) |
| DoF | degrees of freedom |
| EoL | end of life |
| FiT | feed-in tariff |
| MAE | mean absolute error |
| ML | Machine Learning |
| MPP | maximum power point |
| NPV | net present value (€) |
| PDR | production to demand ratio (–) |
| PV | photovoltaic |
| PVB | photovoltaic-battery |
| SCR | self-consumption ratio (–) |
| SDR | storage to demand ratio (–) |
| SSR | self-sufficiency ratio (–) |
| STC | standard testing conditions ($T_{STC}$ = 25 °C, $G_{STC}$ = 1.0 kW/m$^2$) |
| TMY | typical meteorological year |

*Greek symbols*

| | |
|---|---|
| $\alpha_I$ | temperature coefficient of current at STC (%/K) |
| $\alpha_V$ | temperature coefficient of voltage at STC (%/K) |
| $\Delta t$ | time step (s) |
| $\delta$ | PV technology coefficient (–) |
| $\eta_c$ | battery charging efficiency (–) |
| $\eta_d$ | battery discharging efficiency (–) |
| $\eta_{inv}$ | inverter efficiency (–) |
| $\sigma_{CL}$ | effective fraction of battery capacity usable due to cycle life degradation (–) |
| $\Omega_x$ | sampling distribution for $\boldsymbol{x}_{\text{DoF}}$ |

*Symbols*

| | |
|---|---|
| $A_m$ | module surface area (m$^2$) |
| $C_0$ | investment costs (€) |
| $C_i$ | costs in year $i$ (€) |
| $c_{bat}$ | specific battery system costs (€/kWh) |
| $c_{bat}^{\star}$ | replacement cost of battery (€/kWh) |
| $c_{pv}$ | specific PV system costs (€/kWp) |
| $c_{rem}$ | feed-in remuneration (€/kWh) |
| $c_{ht}$ | high tariff electricity cost (€/kWh) |
| $c_{lt}$ | low tariff electricity cost (€/kWh) |
| $E_{bat}$ | battery charging state (kWh) |
| $E_{bat}^{max}$ | upper bound charging state (kWh) |
| $E_{bat}^{min}$ | lower bound charging state (kWh) |
| $E_{bat}^{R}$ | rated battery capacity (kWh) |
| $G$ | total in plane radiation (kW/m$^2$) |
| $G_{STC}$ | in plane radiation under testing conditions (1 kW/m$^2$) |
| $I_{\text{MPP}}$ | module current at MPP (A) |
| $I_{\text{MPP,STC}}$ | module current at MPP and STC (A) |
| $I_{\text{SC}}$ | short circuit current of PV module (A) |
| $I_{\text{SC,STC}}$ | short circuit current of PV module at STC (A) |
| $L$ | snippet length (days) |
| $N$ | number of load profiles/households |
| $N_c$ | number of cycles before EoL is reached |
| $N_T$ | time horizon (years) |
| $P_{DC}$ | DC power of all PV modules (kW) |
| $P_{DC,N_m}$ | DC power of a PV module (kW) |
| $P_L$ | load (kW) |
| $r$ | discount rate (–) |
| $R_i$ | revenues in year $i$ (€) |
| $r_{esc}$ | escalation rate on electricity prices (–) |
| $r_{rem}$ | annual reduction rate for feed-in remuneration rate (–) |
| $r_{om}$ | share of $C_0$ that accounts for operation and maintenance cost (–) |
| $T_{amb}$ | ambient temperature (°C) |
| $t_{ht}$ | daily high tariff hours |
| $t_{lt}$ | daily low tariff hours |
| $T_m$ | module temperature (°C) |
| $V_{\text{MPP}}$ | module voltage at MPP (V) |
| $V_{\text{MPP,STC}}$ | module voltage at MPP and STC |
| $V_{\text{OC}}$ | open circuit voltage of PV module (V) |
| $V_{\text{OC,STC}}$ | open circuit voltage of PV module at STC (V) |
| $W_{B\rightarrow L}$ | energy supplied to load from the battery bank (kWh) |
| $W_{G\rightarrow L}$ | energy supplied to load from the grid (kWh) |
| $W_{PV}$ | energy (DC) produced by the solar panels (kWh) |
| $W_{PV\rightarrow B}$ | energy supplied to battery from the PV modules (kWh) |
| $W_{PV\rightarrow G}$ | energy supplied to grid from the PV modules (kWh) |
| $W_{PV\rightarrow L}$ | energy supplied to load from the PV modules (kWh) |
| $W_L$ | annual energy demand (kWh) |
| $\overline{w}_L$ | daily average electricity demand (kWh) |
| $w_L$ | normalized daily average electricity demand (–) |
| $\overline{w}_L(t_i)$ | daily average electricity demand during hour $i$ (kWh) |
| $w_L(t_i)$ | normalized daily average electricity demand during hour $i$ (–) |
| $\boldsymbol{x}_{\text{DoF}}$ | degree of freedom vector ($P_0$,$E_{bat}^R$) |

## 1. Introduction

Many countries have put forward ambitious targets to increase the share of energy they generate from renewable sources. For instance, the Energy Roadmap 2050 of the European Commission foresees an almost emission-free electricity production in Europe by 2050 [1]. Photovoltaic (PV) systems, which are seen as a cornerstone of these plans, have recently experienced a considerable increase in market diffusion in many countries. Spurred by a rapid price decline with prices for residential PV system falling by over 80% from 2008 to 2016 in most competitive markets [2], solar PV represented almost half of newly installed renewable power capacity in 2016 [3]. As a result, global PV deployment increased from 3.7 GW in 2004 to more than 300 GW at the end of 2016 [4].

Small-scale PV systems on residential or commercial buildings account for about a third of the globally installed PV capacity and generation [5,6]. Owners of small-scale PV systems can either inject the electricity produced into the distribution grid at a feed-in tariff, or self-consume it to cover the building's electricity demand. Adding on-site battery (B) storage to PV systems makes it possible to store PV-produced electricity for later use. Similar to the declining costs of PV modules, the price of lithium-ion batteries has also started to decrease substantially and is expected to follow a similar price decline as that seen for PV panels [7–9]. In particular, for consumers whose production and demand times do not correspond, the addition of battery storage increases the self-consumption ratio (SCR) – the ratio of electricity generated by the PV system that is directly used at the installation site to the total amount of electricity generated [10]. When the generation cost of PV and battery-supplied electricity is below the retail price, self-consumption is favorable from an owner's perspective. In most regions, the remuneration for feeding electricity into the grid was gradually reduced and many policymakers push to remove feed-in tariffs [11]. Consequently, self-consumption has become increasingly attractive in many countries over the past few years due to increasing electricity

prices in the residential sector, decreasing feed-in tariffs, and falling levelized costs of PV-produced electricity [12,10].

However, the installation of a photovoltaic-battery (PVB) system is not equally profitable for all consumers. A household that consumes large amounts of electricity during sunny hours may amortize the investment into a PV system much more quickly than a household with the same annual demand that uses electricity primarily in the evening hours. Previous research suggests that there is large variability in the profitability of these systems even among households that face the same component costs and the same local conditions regarding climate, weather, and electricity rates (grid-supplied electricity and feed-in tariffs) [12–14]. The configuration of the PVB system to achieve the highest profitability depends on consumer-specific parameters, in particular annual electricity demand, orientation and tilting angle of the PV array, and congruence of production and demand [15]. In fact, two households with the same annual demand may require completely different optimal system configurations and achieve very different net present values [16]. Yet, previous research has only partially addressed the heterogeneity of real-world load profiles and its influence on the optimal configuration and economics of PVB systems [17,10]. Many existing studies use synthetic load profile data [18,19,17,20] or average reference profiles [21–23] and thus neglect the variability of households' demand [24].

This article takes the heterogeneity of real-world load profiles into account. To that end, we develop a techno-economic simulation model that uses local weather data and current electricity rates as input to optimize the battery size and installed PV power for each given load profile. In a first step, we analyze for what fraction of households in Zurich, Switzerland, a PVB system is profitable already today. To account for the variability in real-world consumption data, the analysis processes a large set of smart-meter data from 4190 households. In a second step, we conduct a sensitivity analysis with different cost scenarios to investigate how future price reductions of PV and PVB systems affect optimal system configuration and profitability. In a third step, we use the results of the techno-economic optimization method as ground truth to develop and evaluate a machine learning algorithm that predicts system profitability based only on a limited set of input data (annual demand and daily average load profile). In particular, we investigate how shorter timeframes of smart-meter data affect our prediction results for optimal system configuration, self-consumption ratio, and profitability.

## 2. Related work and local market situation

### 2.1. Related work

PVB systems can be understood as key components for decentralized energy systems and have been studied for many years. In many regions, solar PV is approaching or has reached grid parity [25,16]. Costs for battery storage systems have also declined substantially in the past few years [7,9]. These developments have sparked an increased interest in PVB systems. As a result, in addition to the vast body of research that assesses particular technical aspects of specific PVB system components in detail (including ageing of different battery technologies, advances in the efficiency of PV modules or of inverter power electronics), a considerable body of literature provides holistic evaluations of the technical and economic performance of those systems.

The majority of those articles are based on simplified techno-economic models of PVB systems to analyze how various input parameters influence different variables of interest. Different configurations of PV power and battery sizes may serve as input parameters or may be calculated implicitly in the optimization of other variables of interest – most typically, self-consumption ratio, self-sufficiency ratio, or economic performance. Most articles assess system profitability as key variable of interest [15,16,10] and perform discounted cash flows analyses, reporting either the net present value (NPV) or internal rate of return as outcome variable [21,26,27].

While economic factors are pivotal for the adoption and diffusion of residential PVB systems, in many cases, nonmonetary factors may also play an important role in those investment decisions. Aside from environmental or geopolitical aspects that individuals may want to contribute to, many people value the reduced dependence on utility companies and pursue the reassurance of being self-sufficient as a goal of its own [28,25]. Consequently, a considerable number of articles focus on self-sufficiency [29,30] or self-consumption [13,24] as primary variable of interest. Many articles also investigate how these outcome variables are intertwined. In particular, the impact of self-consumption on the economics of PVB systems has a pronounced position in the scientific literature [12]. Luthander et al. [31] recently summarized the previous research in the field of self-consumption of electricity from residential PV systems. The input parameters studied cover a wide range from political boundary conditions on the macro-level (e.g., subsidies, feed-in tariffs), to local weather conditions, technology-related aspects (e.g.,

**Table 1**
Overview of recent related work on PVB-systems.

| Author | Integrated optimization of PV | Load profile type | Number of load profiles | Influence of annual demand on SSR | Influence of annual demand on economics | Influence of profile heterogeneity on SSR | Influence of profile heterogeneity on economics |
|---|---|---|---|---|---|---|---|
| Mulder et al. [38] | Yes | R5 | 7 | No | No | No | No |
| Hoppmann et al. [39] | Yes | R15 | 1 | No | No | No | No |
| Bortolini et al. [40] | Yes | R60 | 1 | No | No | No | No |
| Weniger et al. [15] | No | R1 | 1 | No | No | No | No |
| Tjaden et al. [35] | No | R15 | 74 | No | No | | No |
| Meunier et al. [41] | No | S15 | 6 | Yes | No | No | No |
| Khalilpour & Vassallo [42] | Yes | R60 | 3 | No | No | No | No |
| Khalilpour & Vassallo [16] | Yes | R60 | 6 | No | No | No | Yes |
| Parra et al. [32] | No | R1 | 1 | No | No | No | No |
| Nyholm et al. [13] | Yes | R60 | 2104 | No | No | No | No |
| Beck et a. [12] | Yes | R0.17 | 25 | No | No | No | No |
| Quoilin et al. [24] | Yes | S15 | 894 | No | No | No | No |
| Merei et al. [33] | Yes | R1 | 1 | No | No | No | No |
| Johann & Madlener [34] | No | S? | 10 | No | | No | No |
| Zhang et al. [29] | No | R60 | 1 | No | No | No | No |
| Schopfer et al. [43] | Yes | R30 | 4232 | No | Yes | No | No |
| Linssen et al. [44] | No | S5 | 3 | Yes | No | No | No |
| Bertsch et al. [27] | Yes | R/S30 | 200/200 | Yes | Yes | No | No |
| Present work | Yes | R30 | 4190 | Yes | Yes | Yes | Yes |

system costs, hardware efficiency, type of battery technology), and individual household-level characteristics (e.g., system orientation, annual demand, load shape).

Regarding political boundary conditions, a number of articles assess how electricity retail tariffs [16,32,24,17], interest rates [33,34], and subsidy schemes [27] affect the economic viability of grid-connected residential PVB systems, and others evaluate the role of feed-in tariffs in near- and post-grid parity markets [34,11]. Several studies compare the profitability of PVB systems in different climatic regions and weather conditions within or between countries [35,24,17,27].

Aside from regulatory and climatic conditions, many techno-economic models assess the influence of technology-related aspects. This includes studies that compare the effect of different battery technologies on the economics of PVB systems [36] and a large number of studies that evaluate how different technology cost scenarios affect the economic feasibility of grid-connected PV-battery systems [16,15,33]. While PV systems are increasingly profitable in many regions [31], adding battery storage is not profitable yet for most households under today's cost and tariff conditions. Existing studies differ in their estimates of how far battery prices need to decline to make the addition of battery systems generally profitable. For the context of Germany, for instance, Merei et al. [33] conclude that "even unrealistic battery prices of less than 200 €/kWh cannot lead to an economic solution" (p.177), whereas others find that storage costs of 500–600 €/kWh may already make PVB systems generally profitable in Germany – even in the absence of subsidies [15,37,27].

Aside from the primary variable of interest (optimal system size, self-consumption, self-sufficiency ratio, or economic performance) and the input parameters studied, existing techno-economic models also differ in the methods and input data they use. For an overview, we categorized recently published related work based on the following attributes (Table 1):

- Integrated optimization: classifies whether a techno-economic optimization has been applied to identify the optimal system size (such as PV and battery size), as opposed to an exploratory analysis using different system sizes, tariffs, installation costs, etc.
- Load profile type: indicates whether the analysis is based on real-world profiles (R) or on synthetic load profiles (S) and specifies their temporal resolution. For instance, R15 stands for real load profiles with a temporal resolution of 15 min.
- Number of load profiles that have been analyzed.
- Influence of annual demand on SSR (resp. economics): indicates whether the article evaluates the impact of annual demand on SSR (and economics, respectively).
- Influence of profile heterogeneity on SSR (resp. economics): indicates whether the article assesses how heterogeneity in real-world load profiles influences SSR (and economics, respectively).

As Table 1 shows, there is large variety in the methods and load profile data on which previous studies base their assessments. The load profiles studied vary considerably in their time resolution, an aspect whose importance has been studied by Linssen et al. and Beck et al. [10,12]. While some articles use measurement data from real households, others perform their analyses on synthetic data [18,19,17,20] or average reference profiles [22,23]. Among the studies that use real-world measurement data, many are based only on a single or just a few households. Several researchers have recently pointed out the importance of using realistic consumption data and accounting for the heterogeneity in real-world load profiles: Linssen et al. advise against using aggregated load profiles, as the optimization results may be too optimistic in terms of total costs and required battery size [10]. Likewise, Tjaden et al. [35] and Quoilin et al. [24] emphasize the importance of using realistic load profiles, as aggregated data does not sufficiently reflect the dynamics in the load of individual households, which makes them ill-suited for the assessment of self-sufficiency and self-consumption.

While the list of articles in Table 1 is by no means exhaustive and many other relevant related contributions exist, the table (and this section in general) provides an overview of the ongoing debate and state of research in the field.

### 2.2. Local market situation

The majority of Switzerland's annual electricity demand is covered by hydro power (57%) and nuclear energy (26%). Solar energy covered about 1580 GW h or 2.27% of the total Swiss electricity demand in 2016 [45]. The mean electricity demand per household is 5100 kWh [46]. Like in many other service territories in Switzerland, residential customers in Zurich are subject to a dual time-of-use-tariff structure, with a distinct daytime and nighttime tariff. The average current daytime tariff (6–22 h) is 0.24 € and the nighttime tariff (22–6 h) is 0.14 €. Dual tariffs (or, more generally, time-of-use-tariffs) are not a Swiss particularity, but common in countries like Australia, Canada, Italy, Portugal, the United Kingdom, and USA. In 2018, Switzerland adopted the new energy act by referendum according to which PV producers with installed power smaller than 100 kWp will not receive a guaranteed subsidized feed-in tariff any more. They will continue to receive a remuneration for the electricity they inject into the grid [47], but the local utility company can set and adjust that remuneration rate every calendar year according to current market conditions. An interactive overview of current remuneration rates can be found in [48].

## 3. Data and methodology

### 3.1. Overview

The evaluation of the economic viability of PVB systems depends on various input parameters, both at the level of the individual household (in particular, time-series data on the electricity demand) and regarding local conditions (including weather data and electricity tariffs). Section 3.2 describes the two main sets of input data, namely the load profiles and the preprocessed weather data. In a first step (Section 3.3), we develop a techno-economic simulation model that is able to compute the optimal PV and battery size configuration for a given household and its load profile. For each optimal configuration, the model calculates the net present value along with a set of other output variables (e.g., self-sufficiency and self-consumption ratio). In order to assess how differences in annual demand or how the heterogeneity in real-world load profiles affects the economic viability of PVB systems, a large dataset of load profiles with different consumption patterns is needed. With the ongoing massive rollout of smart meters in many countries, such large datasets with real-world load profiles are increasingly available. In a second step (Section 3.4), we analyze the sensitivity of the outputs of the techno-economic model to different scenarios of future PV and battery costs. The processed dataset produces a large amount of simulation outputs, especially when repeated over different PV and battery system costs. In a third step (Section 3.5), we make use of this large output dataset to develop and evaluate a machine learning algorithm that predicts the NPV and other key output variables based only on a limited set of input data. More precisely, for each of the five output variables of interest, we train an algorithm that predicts the output if only the daily average load profile (24 values) as well as PV and battery costs are known and evaluate the performance of the algorithm for different timeframes on which the daily average load profile is based.

### 3.2. Data

#### 3.2.1. Smart-meter consumption data

While many analyses use synthetic or aggregated load profiles, we take a large dataset of smart-meter data from actual households, which

allows us to take the heterogeneity of real-world load profiles into account. The original dataset contains the electricity demand (in kWh) of 4232 households with a temporal resolution of 30 min. The dataset was collected over 75 weeks between July 10th 2009 and December 26th 2010 in Ireland [49]. The dataset is of high quality: only 42 of the observed households (<1%) have missing datapoints or unrealistic entries, resulting in a dataset with 4190 useful load profiles. The mean annual electricity demand of the sample is 4304 kWh, with a standard deviation of 2164 kWh. The data is anonymous and not tagged with geolocation. The sample of 4190 households contains the following building types: Apartments (1.7%), semi-detached houses (31.7%), detached houses (26.5%), terraced houses (14.5%), bungalow (25.5%), unknown (0.2%).

As Ireland's solar PV installed capacity per inhabitant is the lowest of all EU countries with just over 2 MWp installed in 2015 [50], we decided to transfer the load profiles to Zurich, Switzerland, as a central European country with a more significant share of PV. The choice of Zurich was motivated by the fact that from a regular dialogue with local utility companies and policy makers, the authors are familiar with the regulatory environment and better able to anticipate future developments (for instance, development of feed-in or remuneration tariffs over the next few years). Switzerland had 1394 MWp installed in 2015 [45] and a mean electricity demand per household of 5100 kWh [46], which is comparable to the mean annual demand of the sample (18% higher) and a similar number of sunshine hours throughout the year (see Appendix B.6). The transfer of load profiles from one country to the weather conditions of other countries is common practice in analyses of PV-battery systems [24,51,32].

#### 3.2.2. Preprocessing of weather data

We combine the smart-meter dataset [49] described above with weather data of a typical meteorological year (TMY) for Zurich [52]. The quantities of the TMY data used include direct irradiation, diffuse irradiation, and ambient temperature. For each time step, direct radiation is projected onto the normal vector of the PV panel using modeled azimuth and solar elevation angles [53]. The diffuse radiation is modified by considering that an arbitrary tilted PV module faces only a portion of the hemisphere. The projection of irradiation data onto the tilted surfaces is a common preprocessing step in the analysis of solar systems [53].

### 3.3. Step 1: Techno-economic optimization model

#### 3.3.1. Configuration and operation of the PVB system

PVB systems can be realized in different configurations. The analysis in this study is based on the configuration shown in Fig. (1). The system comprises PV modules, an inverter that converts direct current (DC) into alternating current (AC), and a battery system.

Battery systems can be integrated into the DC or AC circuit. In this study, we assume that the households install the battery in the DC circuit by using hybrid inverters, which can manage direct PV conversion as well as battery charging/discharging. Hybrid inverters are both a cost-effective and efficient choice for PV battery systems, as they ensure high efficiency and do not require the installation of an additional battery inverter or charger.

The battery operation follows a common, straight-forward strategy: it charges whenever surplus solar energy is available and discharges if demand exceeds PV output and the battery is not (almost) empty (see Eq. (A.5)). More precisely, the battery operates between 10% and 90% state of charge levels, which corresponds to a depth of discharge (DoD) of 80%. We assume that the battery can achieve $N_c = 4000$ cycles with 80% guaranteed capacity at its end of life.

#### 3.3.2. Model specification

The techno-economic model maximizes the NPV for each household in the dataset based on a set of input parameters (weather, load profiles, tariffs, physical properties, and component costs). We apply a discounted cash flow analysis, which takes into account incoming and outgoing cash flows, discounted by the discount rate $r$. In line with Hoppmann et al. [39], we set $r$ to 4%. The degrees of freedom (DoFs) for the optimization include battery size and installed PV power for each household, and are summarized in the DoF vector $\boldsymbol{x}_{\text{DoF}} = (E^R_{bat}, P_0)$. The optimization problem for the maximization of the NPV is given by

$$\max_{\boldsymbol{x}_{\text{DoF}}} \text{NPV} = \max_{\boldsymbol{x}_{\text{DoF}}} \left\{ -C_0 + \sum_{i=1}^{N_T=20} \frac{S_i}{(1+r)^i} \right\} \quad \text{with } \boldsymbol{x}_{\text{DoF}} \in \Omega_x \tag{1}$$

where $C_0$ includes the investment costs for both the PV and battery system and $S_i$ denotes the cash flows (or net savings) generated in year $i$. $S_i$ comprises savings resulting from avoided electricity costs by substituting grid-supplied energy with PV-generated energy $W_{PV\to L} + W_{B\to L}$ and profits accruing from electricity injected into the grid at the local remuneration rates. The cash flows $S_i$ take into account expenditures for operation and maintenance, as well as battery replacement costs due to cyclic aging (see Appendix A.4 for a detailed explanation). Appendix A.5 provides a more detailed description of the cash flow model applied.

The NPV is obtained numerically using grid search over the domain $\Omega_x$, which contains discrete power ratings $P_0$ of the PV panel and possible capacities $E^R_{bat}$ of the battery:

$$P_0 = [8,9,\ldots,12,14,16,18,20,30,\ldots,120] \times P_{mod} \quad \text{(in kWp)} \tag{2}$$

$$E^R_{bat} = [0,1,2,3,4,5,6,8,10,12,\ldots,38,40] \quad \text{(in kWh)} \tag{3}$$

$P_{mod}$ is the rated peak power of a single PV module, which is $P_{mod} = 0.260$ kWp. We assume a minimal PV system size of $8 \times P_{mod} = 2.08$ kWp [54]. The set $\Omega_x$ contains $24 \times 24 = 576$ PV and battery combinations in discrete steps. All samples of $\Omega_x$ are forwarded to the techno-economic model, which evaluates the NPV for all 576

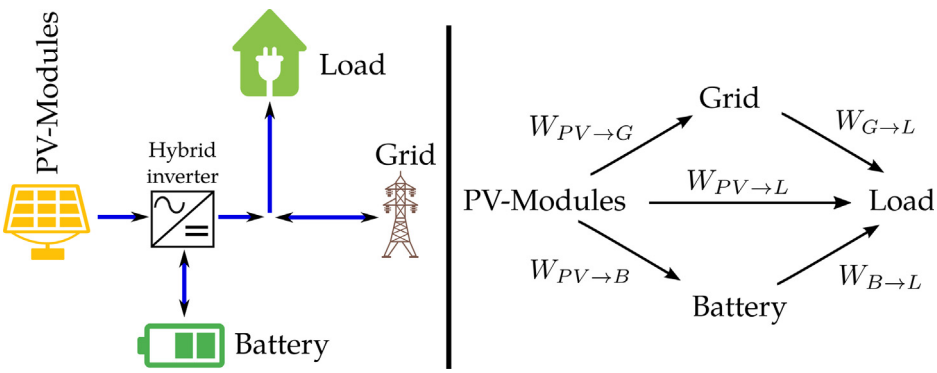


**Fig. 1.** Major components of a PVB system and simplified connection scheme are shown on the left. The right side denotes the annual amount of energy transferred between the components.

combinations. Following Eq. (1), the value for $\boldsymbol{x}_{\mathrm{DoF}}$ that maximizes the NPV is retained. Thus, the model chooses the configuration of battery size and PV array size that optimizes the NPV for any given combination of the input parameters (load profile, weather data, retail tariffs, system costs, etc.).

The system configuration obtained by Eq. (1) is then used to derive the self-sufficiency ratio (SSR), meaning that, annually, an amount of SSR·$W_L$ (in units of kWh) is produced and self-consumed using the PVB system. The remaining portion of (1−SSR)·$W_L$ must be bought from the local grid provider. The self-sufficiency ratio is defined by

$$\mathrm{SSR} = \frac{W_{PV\rightarrow L} + W_{B\rightarrow L}}{W_L} \tag{4}$$

The share of generated solar energy that covers the load directly or via the battery is referred to as self-consumption ratio and defined by

$$\mathrm{SCR} = \frac{W_{PV\rightarrow L} + W_{B\rightarrow L}}{W_{PV}} \tag{5}$$

Therefore, the amount (1−SCR)·$W_{PV}$ (in units of kWh) corresponds to the solar energy injected into the grid.

The optimal PV power and battery size can be normalized with respect to the annual and mean daily demand, respectively. The production to demand ratio (PDR) is the ratio of the net produced solar energy $W_{PV}$ and the annual demand or, more formally

$$\mathrm{PDR} = \frac{W_{PV}}{W_L} = \frac{\mathrm{SSR}}{\mathrm{SCR}} \tag{6}$$

A PDR of 1 is often referred to as net zero energy building [14], which means that over the year the household produces as much energy as it consumes, irrespective of production and demand concurrence.

Battery systems available on the market today typically have a capacity between 1 and 10 kWh for residential applications. The ratio between battery size and daily average demand is an intuitive score. Thus, we define the storage to demand ratio (SDR) as

$$\mathrm{SDR} = \frac{E^R_{bat}}{\overline{w}_L} \tag{7}$$

where $\overline{w}_L = W_L/365$ is the mean daily demand. If the optimization for a household yields a SDR of 1.2, we should size the battery such that it can store 20% more than the daily average demand. The dimensionless ratios are helpful for the comparison of different households and PVB configurations.

### 3.3.3. Techno-economic simulation parameters

The performance of a PVB system depends on a large parameter space, which must be specified prior to running the simulation. Many parameters depend on the local building properties such as available roof surface area, roof orientation, and roof tilting. In addition to the technical system properties, the local weather and the price of the grid-supplied electricity affect the economic performance of PVB systems. All input parameters are specified in Table 2. For a detailed description of the assumptions made, please refer to Appendix A.

The analyzed smart-meter dataset has no reference to the location, roof shape, or orientation of the building. Therefore, the orientation and tilting angle of the PV array are input parameters generated using probability distribution functions for roof orientation and tilting angle. The distributions follow Li et al. [55], assuming a Gaussian distribution (with location = 180°, scale = 50°) for the orientation angle and a Gompertz distribution (location = 0, scale = 12, shape = 0.03) for the tilting angle. The distributions are shown in Fig. 2.

In central European countries, PV systems generate the maximum annual energy output when oriented south with a tilting angle between 20° and 30° [15]. Such configurations are optimal if the produced energy is reimbursed with a constant FiT. Many countries have adopted an FiT policy over the past years. In European countries, FiTs are continuously dropping due to the adjustment to falling PV module prices. In Switzerland, subsidized FiTs for small-scale PV systems (smaller than 100 kWp) were replaced with a cash-bonus-type subsidy in 2018 [62]. This policy shift motivates owners of a PV system to maximize self-consumption and minimize their dependence on remuneration rates. Under this self-consumption policy, the influence of orientation and tilting angle on the self-consumption factor is weaker [15], as the coincidence of load and production is more important than the annual energy output of a PV system. In our simulation, we assume a remuneration rate of 0.068 €/kWh (current Zurich tariff [61]), which is annually depreciating by 10% (utilities are allowed to adjust the remuneration rate annually). This reflects that the remuneration rates are adjusted annually to account for falling PV module prices [63]. To get an unbiased financial perspective on PVB systems, we have entirely neglected such subsidies based on cash bonuses and included a comprehensive sensitivity analysis to account for future PV and battery cost developments. However, the effects of the cash bonus subsidy can be estimated based on the variation of PV costs as explained in the next subsection.

### 3.3.4. Base case cost scenario

Both PV and battey system prices can vary significantly as they depend on local conditions (i.e., difficulty of installation), differences in manufacturer prices, and different margins for suppliers and installers etc. A survey in Switzerland estimated the system prices in 2015 for PV installations and reported a median cost of approximately 2100 €/kWp. The smallest observed system size was 2 kWp [54], which corresponds to the minimal values of the search domain $\Omega_x$ defined in Eq. (2). Based on the survey, we assume 2000 €/kWp as a reasonable price tag for installations as of 2018.

**Table 2**
List of simulation input parameters.

| Input parameter | Adopted value | References |
|---|---|---|
| **Building properties** | | |
| Weather station | Zurich | [52] |
| Orientation | stochastic | [55] |
| Tilt | stochastic | [55] |
| **PV module properties** | | [56] |
| Open circuit voltage and short cut current at STC | | |
| $V_{\mathrm{OC,STC}}$,$I_{\mathrm{SC,STC}}$ | 37.9 V, 8.73 A | |
| Max. power point characteristics | | |
| $V_{\mathrm{MPP}}$,$I_{\mathrm{MPP}}$ | 31.6 V, 8.73 A | |
| Temperature coefficients: $\alpha_I$,$\alpha_V$ | −0.31%/K, 0.06%/K | |
| Module area $A_m$ | 1.63 m$^2$ | |
| **Battery properties** | | [57] |
| Cycle life $N_c$ | 4000 | |
| End of life | 80% of $E^R_{bat}$ at $N_c$ | |
| Depth of discharge DoD | 80% | |
| **Efficiencies** | | [58] |
| Inverter/Charger efficiency $\eta_{inv}$ | 0.95 | |
| Charge/discharge efficiency $\eta_c$,$\eta_d$ | 0.95 | |
| **Economic parameters** | | |
| PV cost scenario $c_{pv}$ | 1000–2500 €/kWp | [54] |
| Battery cost scenario $c_{bat}$ | 250–1000 €/kWh | [27] |
| Battery replacement costs $c^{\star}_{bat}$ | $c_{bat}/2$ | |
| Operating and maintenance costs $r_{om}$ | 0.01 | [59] |
| Discount rate $r$ | 0.04 | [39] |
| Electricity escalation rate $r_{esc}$ | 0.025 | [60] |
| Remuneration rate reduction per year $r_{rem}$ | 0.1 | |
| Project lifetime $N_T$ | 20 years | [59] |
| **Tariffs** | | [61] |
| High tariff periods $t_{ht}$ | 6am to 10 pm (Mo-Sa) | |
| Low tariff periods $t_{lt}$ | otherwise | |
| High tariff costs $c_{ht}$ | 0.240 €/kWh | |
| Low tariff costs $c_{lt}$ | 0.120 €/kWh | |
| Remuneration rate $c^i_{rem}$ | 0.068 €/kWh | |

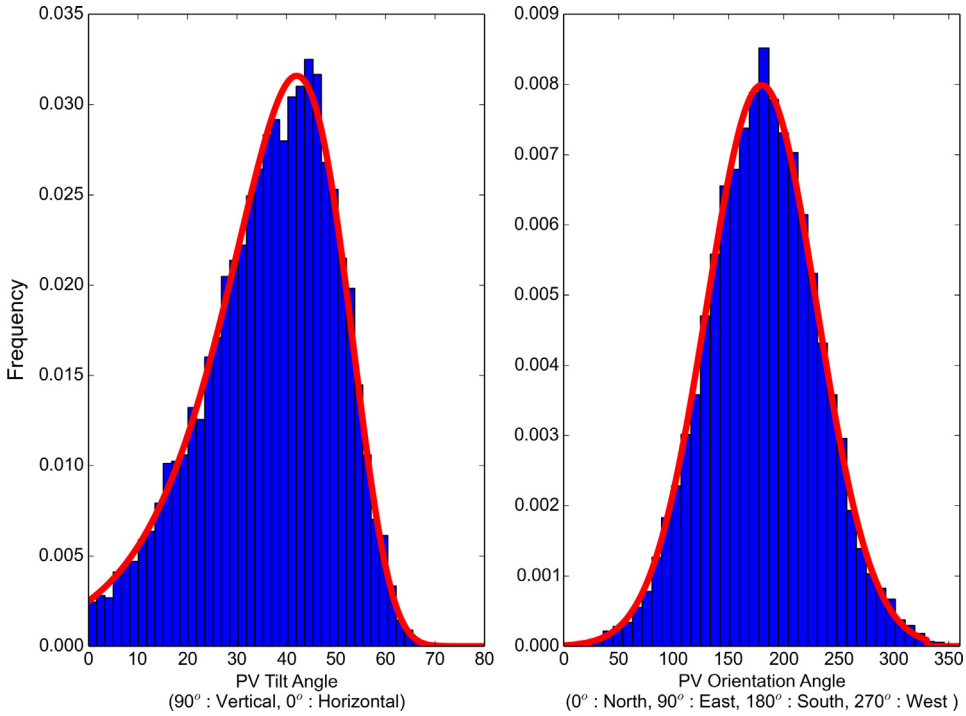


**Fig. 2.** Probability distribution of orientation angle and tilting angle.

The cost variation of battery installations may be just as high as for the PV system itself. Dehler [64] found a variation between 870 and 3200 €/kWh in battery system costs and points out that cell costs alone amount to 300 €/kWh and could fall to 200 €/kWh in 2020 and 150 €/kWh in 2030 [65]. Truong et al. reported battery system costs of 780 €/kWh for a 6 kWh Tesla Powerwall [66]. Single battery systems with a size of 2–3 kWh can already be purchased today for 500 €/kWh (before installation) [67]. Linssen et al. [10] assumed 1000 €/kWh including installation, which we adopt in this study as a base case. Note that the sensitivity analysis introduced in Section 3.4 considers future battery costs as low as 250 €/kWh, which are well below current market prices of 1000 €/kWh.

### 3.4. Step 2: Sensitivity analysis

Future system prices are assumed to further decrease [68,69]. In the last 35 years, the module price decreased by 23% with each doubling of the cumulated module production (cost reductions result from economies of scale and technological improvements) [70]. To account for these future developments, we evaluate the techno-economic model under 16 different PV and battery system cost scenarios. For the PV costs, we chose 1000, 1500, 2000 and 2500 €/kWh. For the battery costs, we applied the same cost variation as Bertsch et al. [71], which ranges from 250, 500, 750 to 1000 €/kWh. Note that the base case cost scenario described in Section 3.3.4 is one of the 16 cost scenarios. The sensitivity analysis resolves the relationship between annual demand and achieved NPV for each cost scenario. In addition to reporting the share of households that achieve profitability in each scenario, we show how the optimized PV power, battery sizes, SSR and SCR are affected by the technology costs.

### 3.5. Step 3: Predictor training and testing

#### 3.5.1. Point of departure

As point of departure, we assume the following situation: a household is considering the installation of a PV or a PVB system. The goal now is to predict – based on the limited set of data that utility companies have available – the optimal PVB configuration of for the given household and its NPV.

In step 1, we used 30-min load curves and TMY weather data to derive the optimal system configuration and the exact resulting system profitability, SCR, and SSR. In the prediction, we now strictly limit the input data to information that is available at the end of the year 2009 as this would be the input the decision maker has available at the time of decision making. The data for 2010 is only used ex post in order to evaluate the quality of the system choice and the accuracy of the prediction of the system's performance.

As input for the predictor for a given household $k$, we use the mean daily consumption of household $k$ and its characteristic daily load curve, both from 2009, as well as the expected PV and battery costs. The daily load curve of household $k$ – we also refer to it as load snippet hereafter – consists of 24 hourly values of the average daily demand. These hourly averages are calculated based on $L$ days of smart-meter data from 2009. We deliberately restrict the timeframe $L$ of the smart-meter dataset to cover between one and 160 days, as most utility companies do not store fine-grained data by default. For the sake of the predictive model's practical applicability, the consumption data needs to be stored only if a customer commissions the configuration and NPV assessment. The predictive model – essentially a regression – needs to be trained before it is being put to use. In order to avoid overfitting, we carefully separated the data into training and test (or evaluation) data and made sure that the model is not built on information that is used to assess its quality in a later step. We apply a ten-fold cross validation for that purpose; additional information of the cross validation procedure can be found in Appendix C.4.1. Fig. 3 illustrates the separation of the input data.

#### 3.5.2. Input and output of the predictive model

In this subsection, we describe how the simulation outputs from step 1 and 2 are used to train and evaluate the predictor; Fig. 4 illustrates the procedure. The outputs from step 1 serve as dependent variables, and the following data serve as input variables (features) of the predictor:

- The normalized daily average load profile (with hourly resolution),

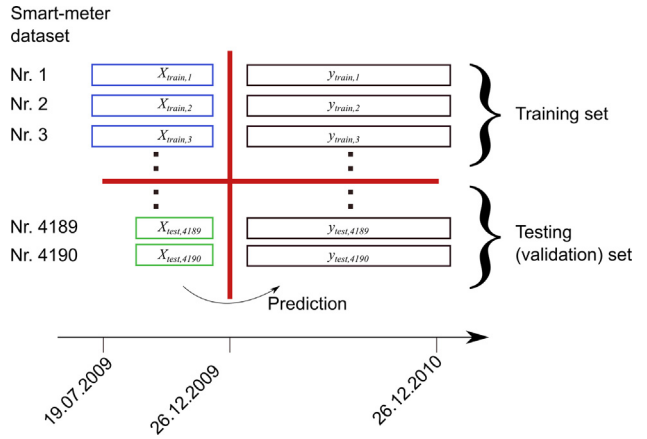


**Fig. 3.** Schematic on test train split and the variable snippet length used as input feature for prediction.

referred to as load shape

- The average daily demand of the 2009 dataset $\overline{w}_L^{(2009)} \approx W_L^{(2009)}/365$
- The specific PV costs $c_{pv}$ (in €/kWp)
- The specific battery costs $c_{bat}$ (in €/kWh)

The load profile and the average daily demand are quantities that can be used if only incomplete smart-meter data (i.e., sampled for less than a calendar year) is available. In this situation, the load shape is computed from the smart-meter data snippet available and passed on to the predictive model, which can then compute the optimal PV and battery size.

The accuracy of the predictor is affected by the quality of the input data (especially by the length of the smart meter data snipped to construct the characteristic load curve). The longer the time frame, the better the estimation of characteristic load shape and the daily average demand. We vary the snippet length between (1,7,14,30,60,90,160) days (always ending end of 2009) and report the error scores for each snippet duration. The total annual demand is a quantity that all utility companies track and store for billing purposes. As we only have about half a year of data for 2009 available, our model input describing the average daily demand for 2009 is less accurate than the input a utility company could use. Thus, the estimates represent a conservative estimate of the predictor's performance. The predictor is more flexible than the techno-economic model from step 1, as it can still provide accurate results even for situations where only incomplete smart-meter data readings (collected for a period much shorter than a year) are available. In addition, the computational burden is greatly reduced, as no extensive grid search for the optimal configuration is performed.

### 3.5.3. Predictive model specification

The four features can be further formalized in the feature matrix $X$. The $k$th sample can be written as

$$X_k = (w_k(t_1), w_k(t_2), \ldots, w_k(t_m), \ldots, w_k(t_{24}), \overline{w}_{L,k}, c_{pv}, c_{bat}) \tag{8}$$

The values $w_k(t_m)$ for $m = 1,2,\ldots,24$ represent the normalized average daily consumption in hour $m$ of the day. The sum of the normalized loads over all hours $t_m$ is $\sum_{m=1}^{24} w_L(t_m) = 1$. The feature vector $X_k$ contains the load shape feature (normalized daily average demand), the daily average demand $\overline{w}_{L,k} = W_{L,k}/365$, the specific PV power costs (in €/kWp), and the specific battery costs (in €/kWh). The function $f$ maps the features $\boldsymbol{X}$ to an output of interest without a mathematical specification of $f$, as opposed to the previous efforts where the function $f$ for a set of input factors has been parametrically defined. We aim to predict the following output variables:

$$y = \{\text{NPV}, P_0, E_{bat}^R, \text{SSR}, \text{SCR}\} \tag{9}$$

The goal is then to construct a regressor $f_i$ that is able to predict the target variable $y_i$ given the feature matrix $\boldsymbol{X}$. Mathematically, this is

$$y_i = f_i(\boldsymbol{X}) \qquad i = 1,\ldots,5 \tag{10}$$

A machine learning algorithm can then be trained on the feature matrix $\boldsymbol{X}$ for each of the five output variables. We use the random forest algorithm to approximate $f_1,\ldots,f_5$, as it can construct nonlinear relations between input features and the outputs and does not require large parametrization efforts [72]. The original model described in Appendix A with its large input parameter space can be represented by a random forest algorithm $f_1,\ldots,f_5$ that implicitly contains all input parameters except for the load shape and average daily demand itself.

Once trained, the feature matrix for testing and validation purposes must be constructed as illustrated in Fig. 5. The first step in this process is the prediction of the NPV. If the NPV is negative, no prediction of the system sizes occurs. If the predicted NPV is positive, we subsequently estimate the optimal system size, the expected SSR and SCR, respectively.

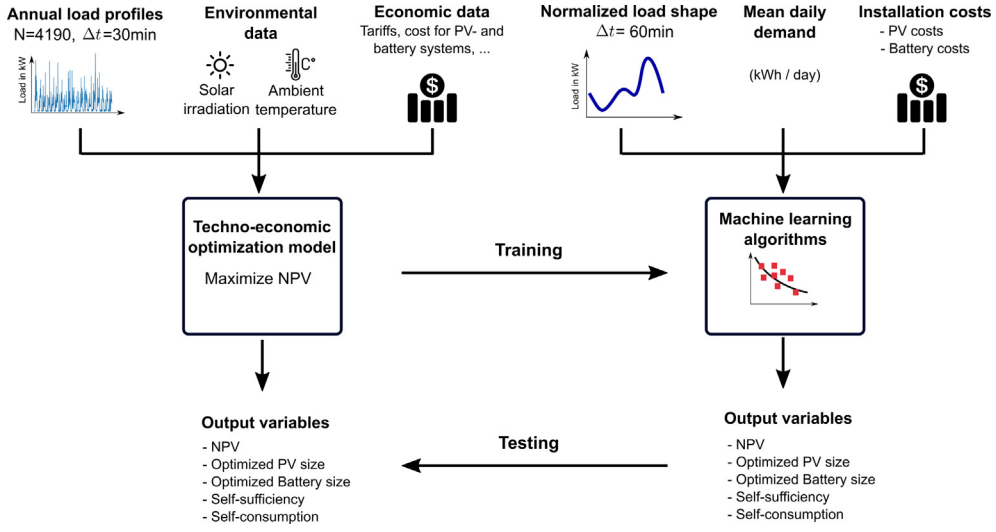


**Fig. 4.** Training of the predictor with the existing simulation outputs.

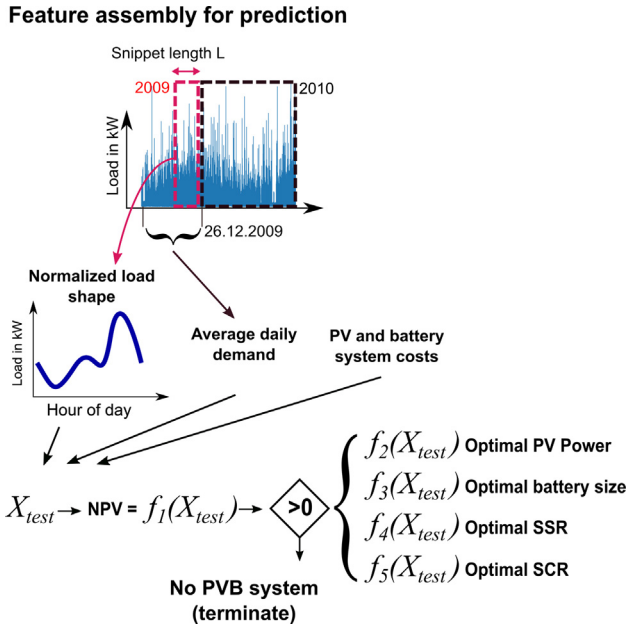


**Fig. 5.** Prediction flow diagram visualizes how the test matrix can be constructed for the prediction.

## 4. Results

### 4.1. Simulation results for the base case scenario

This subsection presents the simulation results for the base case cost scenario of (PV:2000 €/kWp, B: 1000 €/kWh). Fig. 6 displays the NPV as a function of the annual demand, where each of the 4190 dots represents a household. In line with previous studies, the figure indicates a strong correlation between annual demand and NPV, which flattens out around 6000 kWh towards a NPV of about 1500 €. About 40% of the households reach a positive (or zero) NPV. Whereas the mean NPV across all households is negative (-389 €), the mean NPV of the 90th percentile is 1659 €, compared to −2570 € for the 10th percentile. Households in the 90th percentile have a mean annual demand of 7868 kWh, compared to 1440 kWh for the 10th percentile.

The bottom panel of Fig. 6 shows a histogram with the relative frequency of annual demand, where non-profitable (NPV $<$ 0, in blue) and profitable cases (NPV $\geqslant$ 0, in orange) are displayed separately. The first households reach profitability at an annual demand of approximately 3000 kWh. By contrast, almost all households with an annual demand of 7000 kWh reach profitability. In the range between 3000 kWh and 7000 kWh annual demand alone is not sufficient to predict whether a household reaches profitability.

The spread of the datapoints along the y-axis in the upper panel of Fig. 6 already gives a first qualitative impression that there is great heterogeneity in the profitability even among households with a similar annual demand. Fig. 7 provides more detailed quantitative results. In that chart, households are grouped into equidistant bins of similar annual demand (± 250 kWh). The blue lines in the boxplots indicate the median NPV for each bin. The NPV spread between the upper and lower quartile (the ± 25% of the households around the median, depicted by the black boxes) ranges between 2200 and 3000 € within each bin. Thus, the spread of the NPV between the upper and lower quartile within each bin is larger than the variation of the NPV between two neighboring bins. So, while annual demand has a large impact on the system's profitability, it alone leaves a broad range of uncertainty. Hence, for individual investment decisions, other factors – load shape in particular – should be taken into account; we will return to this point in Section 4.3.

### 4.2. Sensitivity studies for different PV and battery costs

The simulation results in the previous section were based on PV installation costs of 2000 €/kWp and battery installation costs of 750 €/kWh. In this subsection, we analyze how different cost scenarios affect profitability, optimal system configuration, self-sufficiency (SSR), and self-consumption ratios (SCR). For this reason, we repeated the techno-economic optimization for 4 × 4 = 16 cost scenarios. We used PV installation costs of 2500, 2000 (base case), 1500 and 1000 €/kWp. As for the battery storage, we adopted the values of 1000 (base case), 750, 500 and 250 €/kWh as already applied by Bertsch et al. [71].

#### 4.2.1. Sensitivity analysis of the NPV

Fig. 8 displays the histograms of the resulting NPVs for the 4190 households for the each of the 4 × 4 cost scenarios, along with the estimate for the concrete proportion of households with NPV $\geqslant$ 0. In that matrix, PV costs decrease from the top to the bottom panels and battery costs decrease from left to right. The base case is depicted in the first picture from the left in the second row. In each of the 16 cost scenarios, the NPV distribution spreads over a range of 6000–7000 € on the x-axis. Lower PV costs cause a substantial shift in the distributions towards the right, considerably increasing the share of households with NPV $\geqslant$ 0. For PV costs of 2000 and 2500 €/kWp, the share of the households that achieve profitability is always below 50%, except for the configuration of (PV: 2000 €/kWp, B: 250 €/kWh), where 60.8% of the households achieve profitability. In the most optimistic case of PV costs (1000 €/kWp), the share of households with NPV $\geqslant$ 0 is always above 94%, independent of battery costs.

Regarding battery costs, reductions from 1000 €/kWh to 750 €/kWh and even to 500 €/kWh barely increase the share of households with NPV $\geqslant$ 0. We can only observe a significant improvement in the share of households that reach profitability for battery costs of 250 €/kWh. This implies that battery costs will only significantly improve the profitability of PV systems once they reach that price range.

Table 3 contains the mean NPV for the top and bottom 10% of households. Depending on the cost scenario, the mean NPV of the top and bottom 10% of the households differs by 2146–2848 €. The table also displays the average annual demand of those households. For all cost scenarios, the annual demand in the bottom 10% for the NPV is about 1440 kWh, while the top 10% NPVs correspond to annual demand of about 7900 kWh.

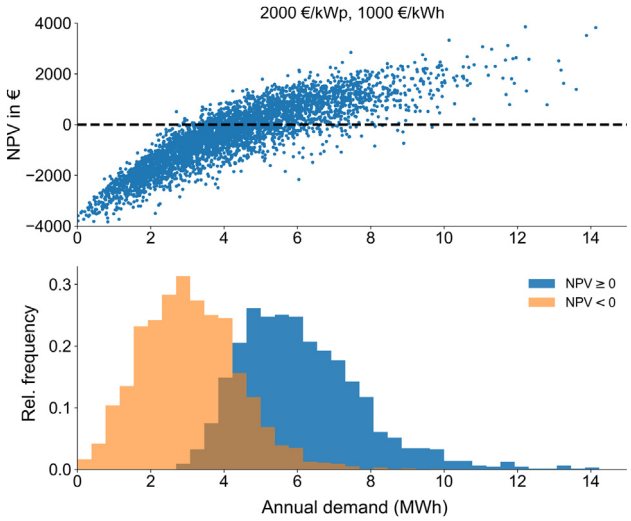


**Fig. 6.** NPV of each household as a function of the annual demand (upper panel) and histograms for profitable (in blue) and non-profitable installations (orange) based on the annual demand. (For interpretation of the references to colour in this figure legend, the reader is referred to the web version of this article.)

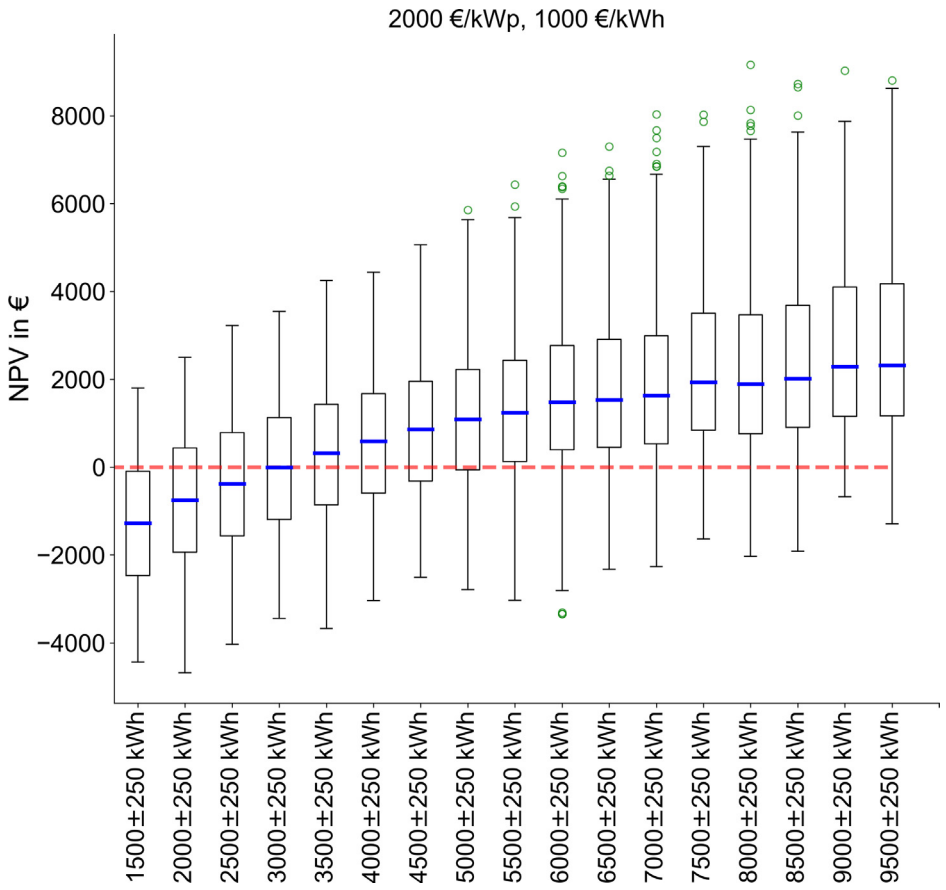


**Fig. 7.** Box plots of the NPV with 500 kWh consumption bins (PV:2000 €/kWp, B: 1000 €/kWh).

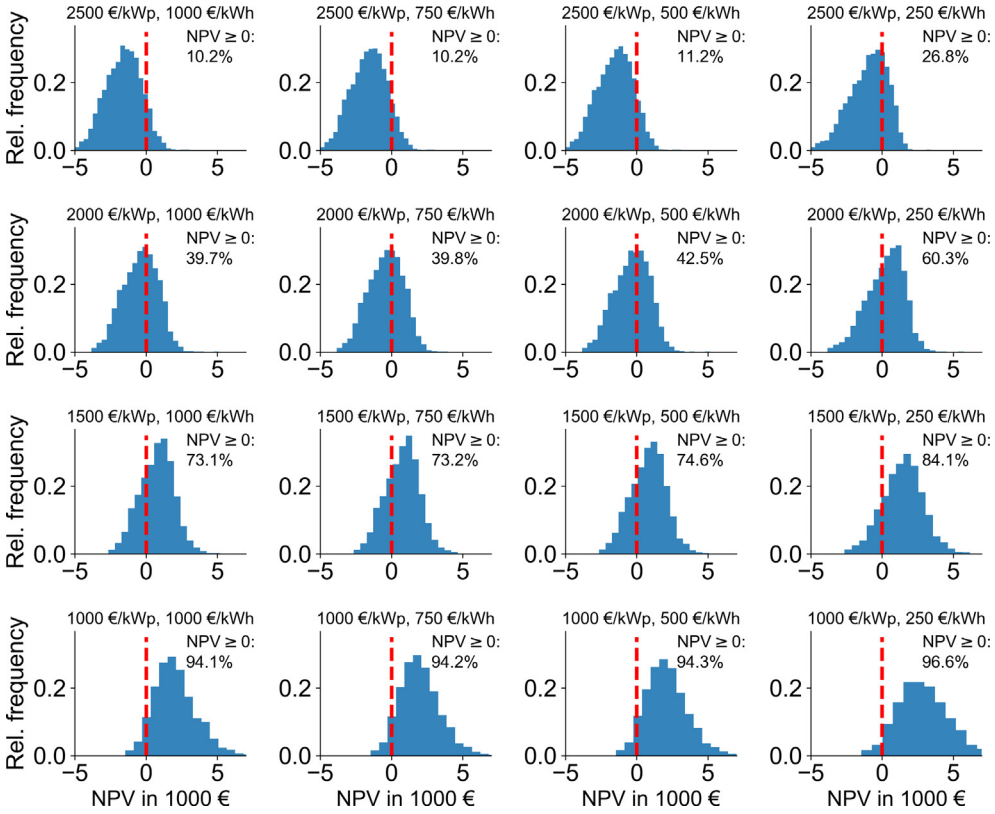


**Fig. 8.** Sensitivity of the NPV distribution to PV and battery system costs.

**Table 3**
Mean NPV for the bottom and top 10% (and mean of all households), along with the annual demand of the top and bottom 10% of the households for each cost scenario.

| PV cost (€/kWp) | Battery cost (€/kWh) | NPV ⩾ 0 (%) | Mean NPV bottom 10% (€) | Mean NPV (€) | Mean NPV top 10% (€) | Demand of bottom 10% NPVs (kWh) | Demand of top 10% NPVs (kWh) |
|---|---|---|---|---|---|---|---|
| 2500 | 1000 | 10.2 | −3761 | −1573 | 545 | 1443 | 7865 |
| | 750 | 10.2 | −3757 | −1568 | 550 | 1440 | 7865 |
| | 500 | 11.2 | −3743 | −1507 | 589 | 1430 | 7854 |
| | 250 | 26.8 | −3468 | −947 | 1058 | 1431 | 7740 |
| 2000 | 1000 | 39.7 | −2574 | −394 | 1656 | 1443 | 7870 |
| | 750 | 39.8 | −2570 | −389 | 1659 | 1440 | 7868 |
| | 500 | 42.5 | −2556 | −331 | 1705 | 1430 | 7826 |
| | 250 | 60.3 | −2281 | 226 | 2291 | 1431 | 7780 |
| 1500 | 1000 | 73.1 | −1387 | 762 | 2911 | 1443 | 7878 |
| | 750 | 73.2 | −1383 | 763 | 2885 | 1440 | 7895 |
| | 500 | 74.6 | −1369 | 824 | 2972 | 1430 | 7883 |
| | 250 | 84.1 | −1094 | 1462 | 4007 | 1431 | 7948 |
| 1000 | 1000 | 94.1 | −200 | 2066 | 5081 | 1443 | 8025 |
| | 750 | 94.2 | −196 | 2030 | 4922 | 1440 | 8048 |
| | 500 | 94.3 | −183 | 2110 | 5041 | 1431 | 8030 |
| | 250 | 96.6 | 83 | 2931 | 6470 | 1423 | 8147 |

#### 4.2.2. Sensitivity analysis of the PV and battery sizes

Each of the cost configurations results in different optimal system sizes. Table 4 provides the resulting mean PV and B sizes (along with their standard deviations) for profitable households. In addition, we report the production to demand ratio (PDR) and the storage to demand ratio (SDR). Fig. C.10 in Appendix C.3 displays the histograms with the PDR and SDR distributions for an additional visual impression. In the base case scenario (PV:2000 €/kWp, B: 1000 €/kWh), the average PV power (among the 40% of the households with NPV ⩾ 0) is 2.2 kWp. The average PDR in the base case is 44% and 54% of the electricity produced is self-consumed. The optimization model computed a battery size greater than 0 kWh only for 0.1% of the households as reported in Table C.8. For battery costs of 750 €/kWh and above, batteries are practically irrelevant for most households, resulting in a mean battery size close to zero. Similar to the NPV, the PDR remains unchanged for a given PV cost when moving from 1000, to 750 and 500 €/kWh. A small but noticeable increase of the PDR can be achieved if the battery costs decrease to 250 €/kWh, which indicates that larger PV systems can be built if storage prices decrease to 250 €/kWh.

Changes in PV costs, on the other hand, have a much bigger impact on most size-related metrics. For instance, a 500 €/kWp reduction compared to the base case increases the average PV size by 0.4 kWp (about 1.5 modules), PDR by almost 40% to 0.61, and reduces SCR from 54% to 44%.

Batteries increasingly become economically viable if PV costs are equal or below 1500 €/kWp. With battery costs of 750 €/kWh, the optimal configuration includes a battery for only 8.7% of the households (again, of the minimum size specified). By contrast, with battery costs of 500 €/kWp the situation fundamentally changes: in that scenario, 95.7% of the households would benefit from the integration of a battery. While the majority of optimal configurations imply only a small battery in that scenario (resulting in a mean size of 1.3 kWh), the mean battery size at battery costs of 250 €/kWp is 7.4 kWh, and the installation would be profitable for every household analyzed.

For all PV costs equal to or higher than 1500 €/kWp, the maximum PDR just crosses the PDR = 1 mark. This implies that from a profitability point of view, households should not produce more than they consume. For PV costs of 1000 €/kWh, the average PDR is just above 1; this means that in those cost scenarios, PV systems should produce as much solar energy on average as the household consumes.

**Table 4**
Mean PV and battery configurations for each cost scenario.

| PV cost (€/kWp) | Battery cost (€/kWh) | Mean (std) of $P_0$ in kWp | Mean PDR (–) | Mean (std) of $E^R_{bat}$ in kWh | Mean SDR (–) | Mean SSR (–) | Mean SCR (–) |
|---|---|---|---|---|---|---|---|
| 2500 | 1000 | 2.1 (0.3) | 0.34 | 0.0 (0.0) | 0.0 | 0.21 | 0.64 |
| | 750 | 2.1 (0.3) | 0.34 | 0.0 (0.0) | 0.0 | 0.21 | 0.64 |
| | 500 | 2.1 (0.3) | 0.34 | 0.7 (0.5) | 0.04 | 0.24 | 0.70 |
| | 250 | 2.2 (0.3) | 0.41 | 4.7 (1.1) | 0.27 | 0.33 | 0.81 |
| 2000 | 1000 | 2.2 (0.4) | 0.44 | 0.0 (0.0) | 0.0 | 0.23 | 0.53 |
| | 750 | 2.2 (0.4) | 0.44 | 0.0 (0.0) | 0.0 | 0.23 | 0.54 |
| | 500 | 2.2 (0.4) | 0.45 | 1.0 (0.4) | 0.06 | 0.27 | 0.62 |
| | 250 | 2.4 (0.6) | 0.54 | 5.8 (1.9) | 0.41 | 0.40 | 0.76 |
| 1500 | 1000 | 2.6 (0.7) | 0.62 | 0.0 (0.0) | 0.0 | 0.26 | 0.43 |
| | 750 | 2.5 (0.7) | 0.61 | 0.1 (0.3) | 0.01 | 0.26 | 0.44 |
| | 500 | 2.6 (0.7) | 0.62 | 1.3 (0.6) | 0.09 | 0.32 | 0.52 |
| | 250 | 2.9 (1.0) | 0.74 | 7.4 (3.3) | 0.57 | 0.50 | 0.69 |
| 1000 | 1000 | 4.0 (1.7) | 1.07 | 0.0 (0.0) | 0.0 | 0.31 | 0.30 |
| | 750 | 3.7 (1.6) | 1.02 | 0.4 (0.5) | 0.03 | 0.32 | 0.33 |
| | 500 | 3.8 (1.6) | 1.03 | 2.0 (1.1) | 0.16 | 0.40 | 0.40 |
| | 250 | 4.4 (2.1) | 1.19 | 9.6 (5.2) | 0.78 | 0.62 | 0.54 |

With regards to self-sufficiency ratio (SSR) and the self-consumption ratio (SCR), we generally observe that the SCR is high for high-cost scenarios (due to the small system sizes) and increases for the cheapest battery cost considered. By contrast, the SCR decreases for falling PV costs. The SSR increases as both PV and battery costs decrease and reaches a maximum mean SSR of 54% in the most optimistic cost scenario. The highest SSR achieved for a household is 80%, as indicated by Fig. C.11 in the Appendix.

### 4.3. Prediction of profitability and optimal system configuration

#### 4.3.1. Predictor performance

In this section we provide the results of the evaluation of the machine learning algorithms described in Section 3.5, regarding their ability to predict the key outcome variables based on only a limited set of input data. Fig. 9 displays the mean absolute errors (MAE) on the left for each outcome variable and the $r^2$ values on the right for different snippet lengths of smart meter data. The detailed error scores as a function snippet length $L$ are also available in Table C.9 in the appendix.

In general, for all outcome variables, the mean absolute error decreases and the $r^2$ value increases with increasing snippet length. The MAE of the NPV decreases from 829 € for a one-day snippet to below 600 € for 30-day snippets. Given to the 6000–7000 € range of observed NPVs (cf. Fig. 8), the ratio of MAE and the NPV spread is on the order of 10%. The $r^2$ already exceeds the 0.5-mark with seven days of measurement data and increases up to 0.88 for a snippet length of $L = 160$.

The MAE for the PV size prediction also decreases rapidly with the snippet length and reaches 0.30 kWp for 30 days of measurement. Thus, the MAE achieved with a 30-day snippet is comparable to the power $P_{mod} = 0.26$ kWp of one module. With a minimal PV size of 2 kWp, the relative error for the smallest system size is about 15%. Increasing the snippet length from 30 days to 160 days increases the $r^2$ of the PV power prediction from 0.6 to 0.75.

The error scores for the prediction of the battery size improve less than for the PV power predictor. The MAE obtained with a 30-day snippet is 0.81 kWh and barely improves even for 160 days of measurement data. That is a rather high value in particular in comparison to the small size of most batteries in the range of 1–3 kWh. Likewise, the $r^2$ increases only little between 0.53 for a 7-day snippet, to 0.6 for a 160-day snippet.

Both the SSR and SCR can be predicted with a MAE smaller than 6% points for a snippet with a minimal duration of 30 days. The $r^2$ values obtained with a 30-day snippet are 0.42 for the SSR and 0.27 for the SCR; with longer periods of measurement data, the $r^2$ for the SSR increases to 0.56 for the SCR to 0.39.

#### 4.3.2. Feature importance

In addition to the error scores, we also provide relative importance, referred to as feature importance for the prediction of the output variables. Table 5 lists all features and their importance for the prediction of all 5 output variables.

Obviously, the relative importance of the different features is subject to the particular cost scenarios studied; nevertheless, the feature importance scores provide an estimate of the relative importance of the different features for the cost scenarios studied. PV costs are the most important feature in the prediction of the NPV (48.5%); mean daily demand and load shape together amount to the same value. The mean daily demand is about twice as important as the load shape in the estimate of the NPV. Battery cost is the least important factor for the NPV, as in many cases household reach profitability without batteries. Not surprisingly, PV costs play an important role (relative importance of 29.2%) in the prediction of the optimal PV power. Battery costs have a strong relative influence on the optimal battery size (67.1%), SSR (50.7%), and SCR (40.5%).

## 5. Discussion

### 5.1. Discussion of findings and implications

As the results of the techno-economic simulation (base case with PV: 2000 €/kWp, B: 1000 €/kWh) show, PV systems are already profitable today for 40% of the households without any subsidies and at today's PV and battery costs, central European weather conditions, and current electricity tariffs. Integrating battery storage, however, is not profitable yet for 99.9% of the households analyzed. The mean PV power that maximizes profitability is rather small (2.2 kWp) and results in a mean self-consumption ratio of 53%. These results are in line with the predictions of Weniger et al. [15] who noted that the optimal PV system size will shrink to small-scale systems with higher self-consumption rates, as the incomes from the feed-in payments will play a minor role in future (p. 87). Annual demand is a key predictor of profitability. As a simple rule of thumb, the installation of a PV systems is profitable for households with an annual demand above 7000 kWh, but not for those below 3000 kWh; in between those two values and thus for a large number of households, the installation may be profitable or not, depending on the load shape and other factors.

Based on the 4190 real-world load profiles analyzed, we find large variability in the NPV and in the optimal system configuration, even for households with a similar total annual demand. These results corroborate the importance of taking into account the heterogeneity of real-world profiles rather than analyzing aggregated or synthetic load profiles [35,24]. The findings also highlight the importance of considering a household's load shape in PVB-related investment decisions a consideration that, to the best of our knowledge, is not part of most profitability assessments of PV(B) systems.

Our simulation model allows policymakers to systematically assess which factors are critical levers for increasing private investments into PVB systems in their region and to predict how future developments like component costs are likely to affect the future diffusion of PVB systems. The results of the sensitivity analysis reveal the large influence

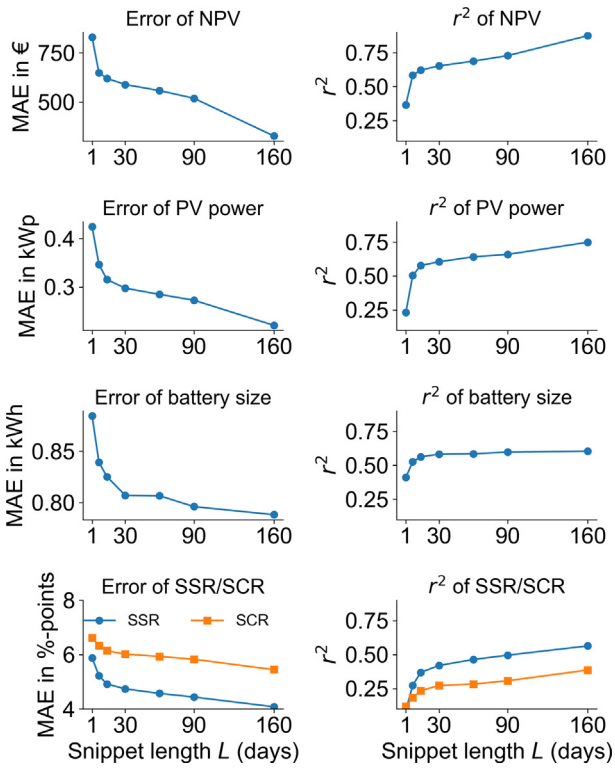


**Fig. 9.** Predictor error and R-squared as a function of snippet length $L$ of smart-meter data.

**Table 5**
Feature importance for all five machine-learning models.

| | Predictor outputs | | | | |
|---|---|---|---|---|---|
| Feature | NPV | PV power | Battery size | SSR | SCR |
| Load shape | 15.8% | 19.8% | 9.7% | 22.0% | 14.2% |
| Mean daily demand | 33.2% | 47.2% | 14.0% | 5.5% | 9.2% |
| PV costs | 48.5% | 29.2% | 9.2% | 21.8% | 36.1% |
| Battery costs | 2.5% | 3.8% | 67.1% | 50.7% | 40.5% |

of PV costs on the share of households that reach profitability. In the most optimistic case of PV costs (1000 €/kWp), the share of households with NPV $\geqslant 0$ is always above 94%, regardless of battery costs. By contrast, batteries can only considerably improve the profitability of PV systems at very small costs close to 250 €/kWh. Once battery costs decrease to that price range, a tipping point is reached: for almost all households, the optimal configuration then comprises a small battery, which increases the mean self-consumption ratio by another 8–22%.

Assuming that all households with NPV $\geqslant 0$ install the optimal system, depending on the cost scenario, the total share of grid-supplied energy would be reduced by 9% in the base case, by 29% in the most optimistic cost scenario for PV (1000 €/kWp), and up to 60% in the most optimistic cost scenario for both technologies (PV: 1000 €/kWp, B: 250 €/kWh). Such a scenario has fundamental implications for infrastructure-related decisions that require long amortization periods such as transregional high-voltage transmission lines.

To the extent that households base their investment decisions on the expected profitability, the results of the sensitivity analysis provide an estimate for the diffusion of PVB systems and of the size of those systems depending on PV and battery costs.

In practice, a complete dataset with detailed smart-meter data readings over a full year is often not available for PVB investment decisions. Therefore, we trained a machine learning algorithm that is able to predict system profitability and other key variables of interest based on much less input data than the techno-economic optimization model, whose output data serve as ground truth. The results show that it is possible to predict a household's optimal PVB configuration and profitability with good accuracy from its averaged daily load profile; in particular, good prediction results can already be achieved when the average daily load profile is based on short timeframes of smart-meter data collection. When historic data on the household's annual demand is available, already with a 30-day snippet of smart meter data the NPV can be predicted with a mean average error below 600 € and a $r^2$ of 0.65; with 160 days of smart meter data, the $r^2$ increases to 0.88 and the mean average error to 328 €. A single month of smart meter data is sufficient to predict the optimal PV power with a mean average error equivalent to the size of about a single module. Thus, the predictions can provide a helpful indication for consumers on how large their PV system or battery should be to optimize profitability.

Our prediction algorithm provides a simple assessment tool for households to individually determine their optimal system configuration and to forecast its profitability. Today, investment decisions for PV (B) systems are often not data-driven, leaving many prospective prosumers without reliable estimates on profitability and system sizing. Our prediction algorithm could mitigate this lack of a data-based decision support system. Based on a limited set of input data (average daily profile based on a few weeks of data collection), it can provide a decent estimate of the optimal configuration, profitability, and self-sufficiency rate and thus, a much better basis to make the investment decision. In addition, the predictor could be used re-estimate the performance if new and heavy electricity load (like EVs or heat pumps) are introduced in the household. Utility companies could use already existing smart-meter data to identify relevant households for whom the installation of a PV(B) system would be profitable. This would allow them to focus their PVB-related marketing campaigns on high-net-worth customers and to better target their communication. This could improve not only the cost-effectiveness of their marketing efforts, but also customer loyalty and sales.

### 5.2. Limitations and outlook

The results are subject to the choice of input parameters and environment studied. First of all, the numbers are based on the assumption that tariffs for grid-supplied electricity are fairly stable (with a moderate 2.5% increase every year) and that the households' annual demand is stable. Future load profiles might be subject to significant changes, due to the diffusion of EVs and the substitution of oil heating systems with heat pumps.

Another limitation is the transfer of load profiles from Ireland to the local conditions of Switzerland. As discussed in Section 3.2 and in Appendix B.1, the two countries are similar with respect to annual electricity demand and daily sunshine hours. Nevertheless, given the slightly more continental climate in Switzerland, one might on average expect more seasonal variation in Swiss load profiles, at least in the 7% of the households with electric space heating.

Extending the model to include thermal (hot water) storage systems would allow for calculating optimal ratios of battery and thermal storage systems. Furthermore, these applications may substantially increase the yearly demand of many households in the future. Since the current model assumes a stable annual demand, our results for system profitability are rather conservative.

Moreover, the dual tariff structure in place in the local context studied – with its pronounced difference between daytime and night time tariffs – the electricity consumed during night hours does not contribute positively to the profitability of the battery. In countries with a flat (and high) electricity tariff, battery storage is likely to be more profitable. The model proposed in this contribution, however, can be easily adjusted to reflect such tariff regimes.

In reality, other aspects are likely to play a role in the investment decision: on the one hand, people may decide to install a system that is unprofitable from today's perspective to reduce their dependence on utility companies [28], or to hedge against the risk of anticipated electricity price increases. The decision to install a PV system may also be driven by nonmonetary reasons: Social interactions (peer effects and spatial knowledge spillovers) have been shown to influence the decision of installing a PV system [73]. People might also value the possibility to publicly signal their pro-social engagement and contribution to pro-environmental causes [74]. On the other hand, consumer inertia, search costs, and uncertainty may prevent people from taking the action necessary to install a profitable system.

The techno-economic model developed in this study has been deliberately designed in a simple way and considers only fundamental physical processes. While parts of the model might be expanded, the current version allows for a techno-economic bottom-up estimation of optimal system configurations and profitability and allows for systematically examining sensitivities of the system profitability to various input factors. Moreover, the current model does not take into account shadowing from trees or neighboring buildings. Depending on the environment of a PV system, the actual solar production may be lower. Moreover, the model assumes that sufficient rooftop space for the installation of the optimal PV size is available, which may not be the case in reality. Future analyses should validate the solar production calculated by the model with real-world PV production data.

Another interesting avenue to pursue is the assessment of increased battery cycle life. Differences in cycle life between different battery technologies and manufacturers depend on the depth of discharge (DoD). The simple battery model presented here could be extended to account for complex degradation effects to assess the influence of cycle life on PVB economics and optimized charging algorithms that adapt to user consumption patterns could be taken into account to minimize battery degradation.

The model could also be expanded to reflect more complex configurations. Secondary applications like providing arbitrage and reserve [75–77] or an integrated energy dispatch of thermal energy and electricity have been shown to improve the profitability for battery systems [78], which could be included in the future.

## 6. Conclusions

We developed a techno-economic model that identifies the optimal configuration of PVB systems under consideration of the heterogeneity of electricity consumption profiles. To account for the heterogeneity in real-world load profiles, we used smart-meter data from 4190 households. The model computes the profitably as well as additional key performance variables including self-sufficiency ratio (SSR) and self-consumption ratio (SCR). Furthermore, we explored how different scenarios of future PV and battery costs affect optimal systems choice and performance indicators. To enable utility companies to identify households among their customers that can reap financial benefits from a PVB system, we have also proposed and evaluated a predictor that identifies such customers and estimates several key outcome variables based only on a limited set of input data, more precisely, on the total annual demand and average daily load profiles.

The results of the techno-economic model reveal high variability in the profitability and in the optimal system configuration, even for households with a similar total annual demand, which highlights the importance of taking into account a household's individual situation in investment decisions. In the central European context studied and without subsidies, we find that PV(B) configurations that optimize profitability will generally not include battery storage in the near future. For PV-systems with batteries to become profitable at population scale, substantial decreases in battery costs (towards a price range of 250–500 €/kWh) would be necessary; even then, small battery sizes will be most profitable to implement. Depending on future costs of PV and battery storage, PVB systems may considerably reduce the demand of grid-supplied energy in the future, which raises the question how fairly allocate contributions to the grid infrastructure in the future.

Finally, the evaluation of our prediction algorithms shows that the profitability of a PVB system and other key variables of interest can be estimated with decent accuracy even for situations where only limited smart-meter data are available. The approach provides a simple and praxis-relevant tool for households to individually assess their optimal system configuration and to forecast its profitability. It also enables utility companies to use already available smart-meter data to identify customers for whom the investment into a PV(B) system is particularly profitable. Thus, the results exemplify how utility companies can use smart-meter data analytics to provide more personalized and customer-oriented services.

## Acknowledgements

The authors would like to express their sincere gratitude to the anonymous reviewers for their valuable suggestions and to Elgar Fleisch (Professor of the Chair of Information Management) for his precious guidance and support. The manuscript benefited greatly from helpful discussions with Marius Schwarz and several other members of Volker Hoffmann's Group for Sustainability and Technology at ETH Zurich, as well as with Reto Flückiger (ABB Corporate Research, Switzerland).

## Appendix A. Techno-economic model

### A.1. Key assumptions for the analysis

This subsection provides further details on the underlying assumptions made for the techno-economic model. Our aim is to keep model complexity low by simplifying the physical processes in the PV modules, batteries, and inverters. However, we also make several assumptions regarding the combination of different data sources used, which are then processed using the model. The following list summarizes the assumptions made in this paper:

A. Each load profile is assumed to represent an individual household.
B. All households are assumed to be located in Zurich, Switzerland.
C. The dataset has been cropped from 26.12.2009 to 26.12.2010 to represent one full calendar year.
D. Each building is characterized by one orientation and tilting angle tuple (randomly assigned based on the distributions shown in Fig. 2). We further assume that the optimal panel size – calculated in step 1 – can always be accommodated on the roof of the consumer's building.
E. The PV modules and PV field experience no partial shadowing.
F. No losses (voltage drops) occur due to wiring between the major components.
G. Battery discharging rates are not limited by the nominal power of the inverter.
H. Changes in state of charge occur continuously within the time step $\Delta t$.
I. Inverter and battery charging/discharging efficiencies are assumed to be constant.
J. Battery degradation depends on the total energy throughput that can be derived by the cycle life numbers issued by the manufacturers.

### A.2. PV module modeling

The power output of a PV module is obtained by a simple state translation model, which is driven by local irradiation and temperature conditions. The description of the state translation model outlined in this subsection is based on Paulescu et al. [53].

A PV module is usually described by several voltage and current characteristics provided by the manufacturer. At any time step $k$, any voltage-current pair on the characteristic curve ($V_{\mathrm{STC}}$,$I_{\mathrm{STC}}$) under standard testing conditions (STCs) can be translated from the STC to any outdoor condition using

$$V^k = V_{\mathrm{STC}}\left(\frac{V_{\mathrm{OC}}^k}{V_{\mathrm{OC,STC}}}\right) \tag{A.1}$$

$$I^k = I_{\mathrm{STC}}\left(\frac{I_{\mathrm{SC}}^k}{I_{\mathrm{SC,STC}}}\right) \tag{A.2}$$

where the expressions for the translated open-circuit voltage $V_{\mathrm{OC}}^k$ and the translated short-circuit current $I_{\mathrm{SC}}^k$ to outdoor conditions are given by

$$V_{\mathrm{OC}}^{k} = \frac{V_{\mathrm{OC,STC}}}{(1 + \alpha_V (T_{STC} - T_m^k))\left(1 + \delta \cdot \ln\frac{G_{STC}}{G^k}\right)} \tag{A.3}$$

$$I_{\mathrm{SC}}^{k} = \frac{I_{\mathrm{SC,STC}}}{1 + \alpha_I (T_{STC} - T_m^k)} \frac{G^k}{G_{STC}} \tag{A.4}$$

PV modules operate sufficiently close at the maximum power point (MPP) using inverter-integrated MPP trackers. Thus, the assumption that each panel is operating at the MPP is applied to Eqs. (A.1) and (A.2). Using this assumption, the pair $(V_{\mathrm{STC}}, I_{\mathrm{STC}})$ can be substituted with $(V_{\mathrm{MPP,STC}}, I_{\mathrm{MPP,STC}})$. The efficiency of PV modules increases at lower module temperatures $T_m$, which can be modeled using $T_m = T_{amb} + C_t \cdot G$ with $C_t = (45\,^{\circ}\mathrm{C} - 20\,^{\circ}\mathrm{C}) / 800\mathrm{W/m^2} = 0.031\,^{\circ}\mathrm{C \cdot m^2/W}$ for any time step $k$ (further details on the temperature coefficient $C_t$ can be found in [53]). The power output of $n$ equally oriented modules at any time step $k$ is then obtained by $P_{DC}^k = n \cdot P_{DC,N_m}^k = n \cdot V^k I^k$. The empirical technology factor $\delta$ can be used to account for different PV technologies. The simulation assumes a mono-crystalline PV technology with $\delta = 0.085$ [53].

### A.3. Battery energy balance

Considerable literature is available on various battery models [79]. Many of these models describe charge, mass, and chemical species transport on the cellular level [80]. However, this study aims to reveal insights on the degree of self-sufficiency and profitability of various customer groups. For that purpose, a simple linear energy balance model is developed. Given a load profile $P_L^k$ at time step $k$, the energy balance reads,

$$E_{bat}^{k+1} = \begin{cases} \min(E_{bat}^k + \Delta P^k \eta_c \Delta t, E_{bat}^{max}) & ,\Delta P^k \geqslant 0 \\ \max(E_{bat}^k + \Delta P^k \eta_d^{-1} \Delta t, E_{bat}^{min}) & ,\Delta P^k < 0 \end{cases} \tag{A.5}$$

where the quantity $\Delta P^k = P_{DC}^k - P_L^k \cdot \eta_{inv}^{-1}$ describes the difference between local production $P_{DC}^l$ and load $P_L^l$ (before the inverter). The situation $\Delta P^k > 0$ represents the case where the solar production exceeds the demand. Depending on the state of charge of the battery, surplus energy may be stored in the battery (direct coverage with production is prioritized over battery discharging). If the demand matches the production $\Delta P^k = 0$, the state of charge of the battery remains unchanged within a time step. The battery may be discharged if the local production is not large enough to cover the load, which is described by the condition $\Delta P^k < 0$. The usable battery capacity given by the interval $[E_{bat}^{min}, E_{bat}^{max}]$ depends on DoD and the residual battery capacity due to cyclic aging. Throughout this study, we assume that the battery capacity fades out linearly until it reaches the end of life (EoL) at 80% of its original capacity. This implies that the fraction of the effectively usable battery capacity due to fading out can be approximated as the average between 100% and 80% of the battery capacity and is given by $\sigma_{CL} = 1 - (1 - 0.8)/2 = 0.9$. The interval of the effectively usable battery capacity over its lifetime is given by $[E_{bat}^{min}, E_{bat}^{max}] = E_{bat}^R \cdot \sigma_{CL} \cdot [1 - \mathrm{DoD}/2, \mathrm{DoD}/2]$

At each time step, the energy flows between the major components – PV modules, batteries, grid, and load – can be described by Eqs. (6)–(10). By summing up over all time steps, annual energy flows can be obtained as illustrated in Fig. 1.

$$W_{PV \to B} = \sum_k W_{PV \to B}^k = \sum_k \max(E_{bat}^{k+1} - E_{bat}^k, 0) \tag{A.6}$$

$$W_{PV \to G} = \sum_k W_{PV \to G}^k = \eta_{inv} \cdot \sum_k \max\left(\Delta P^k \Delta t - \frac{W_{PV \to B}^k}{\eta_c}, 0\right) \tag{A.7}$$

$$W_{B \to L} = \sum_k W_{B \to L}^k = \sum_k \max(-(E_{bat}^{k+1} - E_{bat}^k) \cdot \eta_d \eta_{inv}, 0) \tag{A.8}$$

$$W_{PV \to L} = \sum_k W_{PV \to L}^k = \sum_k (P_L^k \Delta t + \min(\Delta P^k \Delta t, 0) \cdot \eta_{inv}) \tag{A.9}$$

$$W_{G \to L} = \sum_k W_{G \to L}^k = \sum_k (P_L^k \Delta t - W_{PV \to L}^k - W_{B \to L}^k) \tag{A.10}$$

The quantities $W_{PV \to B}, W_{PV \to G}, W_{B \to L}, W_{PV \to L}$, and $W_{G \to L}$describe the annual energy transferred between the PV modules ($PV$), the battery ($B$), the grid ($G$), and the load ($L$) respectively.

### A.4. Battery aging

Batteries are subject to cyclic aging, which is a complex nonlinear function of the battery operation itself and depends on the battery chemistry, and therefore, on DoD, charging rates, charging currents, charging voltage, etc. Since this paper makes no assumption on the underlying battery chemistry used, a simplified approach to determine the EoL of the battery is chosen. Assuming that battery life depends on the total energy throughput [81,82], the point in time of the theoretical EoL can be calculated using

$$t_{EoL} = \frac{E_{bat}^R \cdot \sigma_{CL} \cdot N_c \cdot \mathrm{DoD}}{W_{B \to L}} \tag{A.11}$$

where $W_{B \to L}$ is the energy supplied to the load from the battery per year. Throughout this paper, a fixed cycle number of $N_c = 4000$ with a DoD of 80% is assumed; self-discharging of the battery has been neglected [81].

### A.5. Cash-flow modeling

The economic viability of a PV battery system can be assessed using the discounted cash flow method. The profitability of an investment in a PVB system can be expressed using the NPV, which depends on the investment costs $C_0$ and the costs $C_i$ and revenues $R_i$ in year $i$:

$$\mathrm{NPV} = -C_0 + \sum_{i=1}^{T} \frac{\mathrm{S}_i}{(1+r)^i} = -C_0 + \sum_{i=1}^{T} \frac{(R_i - C_i)}{(1+r)^i} \tag{A.12}$$

$$C_0 = c_{pv} \cdot P_0 + c_{bat} \cdot E_{bat}^R \tag{A.13}$$

$$C_i = c_{lt}(1+r_{esc})^i \cdot \sum_{k \in t_{lt}} W_{G\to L}^k + c_{ht}(1+r_{esc})^i \cdot \sum_{k \in t_{ht}} W_{G\to L}^k + C_0 \cdot r_{om} + \begin{cases} c_{bat}^{\star} \cdot E_{bat}^R, & i = z \cdot \mathrm{int}(N_T/t_{EoL}) \ \forall\, z \in \mathbb{N} \\ 0, & \text{otherwise} \end{cases} \tag{A.14}$$

$$R_i = c_{lt}(1+r_{esc})^i \cdot \sum_{k \in t_{lt}} W_L^k + c_{ht}(1+r_{esc})^i \sum_{k \in t_{ht}} W_L^k + c_{FiT}(1-r_{rem})^i \cdot W_{PV\to G} \tag{A.15}$$

The investment costs (Eq. (A.13)) include the total system cost (hardware plus installation) for both the PV and battery systems. The avoided costs $S_i$ represent the difference between grid supplied energy cost and the self supplied energy saved. With increasing system size (and therefore $C_0$) every household reaches a limit where $S_i$ might not increase sufficiently despite increasing $C_0$ in order to reach a NPV $\geqslant 0$.

The quantity $\sum_{k \in t_{lt}} W_{G\to L}^k$ returns the amount of the grid-supplied energy consumed during low-tariff hours. Accordingly, the function $\sum_{k \in t_{ht}} W_{G\to L}^k$ returns the amount of the grid-supplied energy consumed during high-tariff hours. The same formalism is applied to compute the consumption without the PVB system for low-tariff hours $\left(\sum_{k \in t_{lt}} W_L^k\right)$ and high-tariff hours $\left(\sum_{k \in t_{ht}} W_L^k\right)$, respectively. The battery may be subject to multiple replacements at a cost of $c_B^{\star} \cdot E_{bat}^R$. The revenues are understood as the costs the consumer would incur without installing a PVB system, while the costs are modeled as the grid-supplied energy with a PVB system plus operating and maintenance cost ($C_0 \cdot r_{om}$) and battery replacement costs ($c_{bat}^{\star} \cdot E_{bat}^R$). Additional revenues are generated through grid-injected electricity reimbursed at a rate of $c_{FiT}$.

## Appendix B. Data sources

### B.1. Comparison of climate and weather conditions in Ireland and Switzerland

The following two tables compare average local conditions for Dublin, Ireland, and Zurich, Switzerland, which may affect PV production and household electricity consumption. Comparison of daily sunshine hours in Dublin (Ireland) and Zurich (Switzerland) [83].

See Table B.6.

**Table B.6**
Average daily sunshine hours by month.

| Month | Jan | Feb | Mar | Apr | May | June | July | Aug | Sept | Oct | Nov | Dec |
|---|---|---|---|---|---|---|---|---|---|---|---|---|
| Zurich | 2 | 3 | 4 | 5 | 6 | 6 | 7 | 7 | 5 | 3 | 2 | 1 |
| Dublin | 2 | 3 | 4 | 5 | 6 | 6 | 6 | 5 | 4 | 3 | 2 | 1 |

Comparison of day length and average temperature in summer and winter in Dublin (Ireland) and Zurich (Switzerland) [83,84]. Note that sunset and sunrise times are indicated for 15 Jan. and 15 July.

See Table B.7.

**Table B.7**
Day length and average temperature in summer and winter.

| | Location | Sunrise | Sunset | Day length (h) | Average temperature (°C) |
|---|---|---|---|---|---|
| January | Zurich, CH | 8:13 | 16:45 | 8:32 | 2 |
| | Dublin, IE | 8:32 | 16:36 | 8:04 | 5 |
| July | Zurich, CH | 5:44 | 21:18 | 15:34 | 19 |
| | Dublin, IE | 5:15 | 21:45 | 16:30 | 16 |

## Appendix C. Complementary tables and graphs

### C.1. Battery sizes

See Table C.8.

**Table C.8**
Relative frequency of battery sizes by cost scenario for profitable households (NPV ⩾ 0).

| PV cost | Battery cost | Battery size in kWh | | | | |
|---|---|---|---|---|---|---|
| (€/kWp) | (€/kWh) | 0 | 1 | 2 | 3–10 | >10 |
| 2500 | 1000 | 100.0% | 0.0% | 0.0% | 0.0% | 0.0% |
| | 750 | 99.8% | 0.2% | 0.0% | 0.0% | 0.0% |
| | 500 | 27.7% | 71.5% | 0.6% | 0.2% | 0.0% |
| | 250 | 0.0% | 0.6% | 3.2% | 96.2% | 0.0% |
| 2000 | 1000 | 99.9% | 0.1% | 0.0% | 0.0% | 0.0% |
| | 750 | 99.3% | 0.7% | 0.0% | 0.0% | 0.0% |
| | 500 | 8.7% | 85.9% | 5.3% | 0.1% | 0.0% |
| | 250 | 0.0% | 0.4% | 2.5% | 95.8% | 1.3% |
| 1500 | 1000 | 99.9% | 0.1% | 0.0% | 0.0% | 0.0% |
| | 750 | 91.2% | 8.7% | 0.1% | 0.0% | 0.0% |
| | 500 | 4.3% | 69.4% | 23.4% | 2.9% | 0.0% |
| | 250 | 0.0% | 0.3% | 3.3% | 83.4% | 13.0% |
| 1000 | 1000 | 99.7% | 0.3% | 0.0% | 0.0% | 0.0% |
| | 750 | 64.1% | 33.8% | 2.1% | 0.0% | 0.0% |
| | 500 | 4.1% | 33.7% | 32.8% | 29.4% | 0.0% |
| | 250 | 0.1% | 1.3% | 3.1% | 59.9% | 35.6% |

### C.2. Sensitivity of production to demand ratio (PDR) and storage to demand ratio (SDR)

See Fig. C.10.

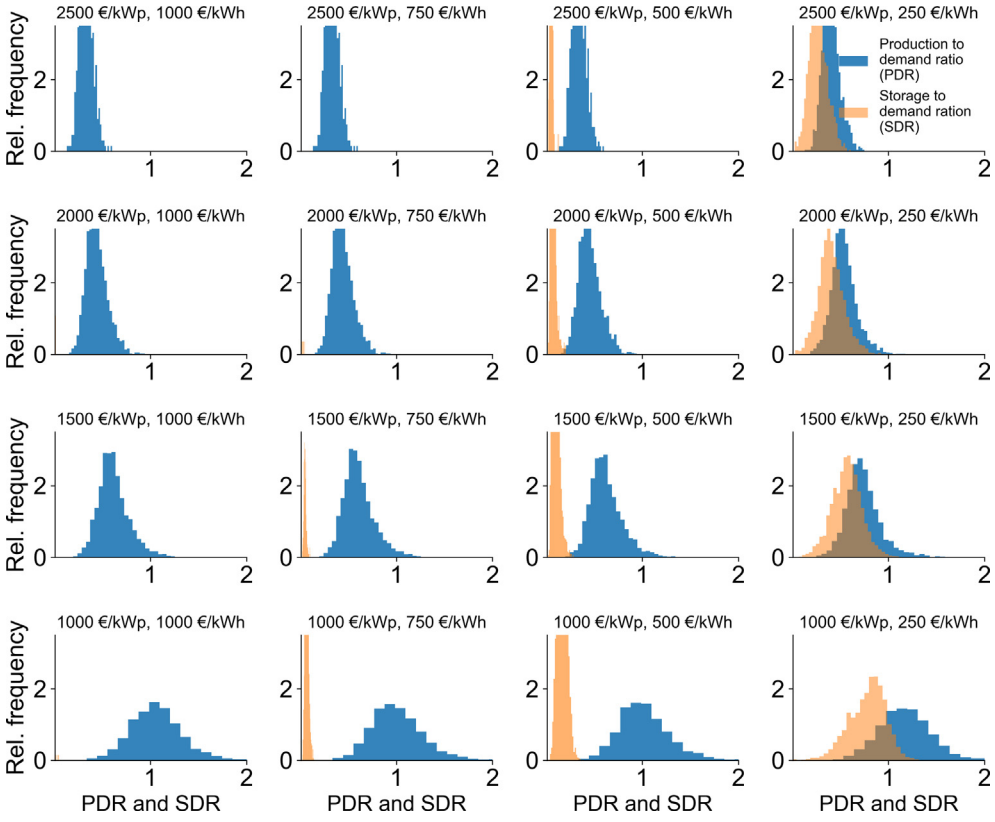


**Fig. C.10.** Distribution of production to demand ratio (PDR) and storage to demand ratio (SDR) in different PV and B cost scenarios.

### C.3. Sensitivity of self-sufficiency (SSR) and self-consumption ratios (SCR)

High installation costs for PV and battery systems result in small PV array sizes (mostly with no battery). In the most expensive cost scenario considered (PV: 2500 €/kWp, B: 1000 €/kWh), this results in high SCRs, but low SSRs, as the histograms in the first panel in Fig. C.11 indicate. The resulting mean values for SCR (64%) and SSR (21%) are also reported in the first line of Table 4.

See Fig. C.11.

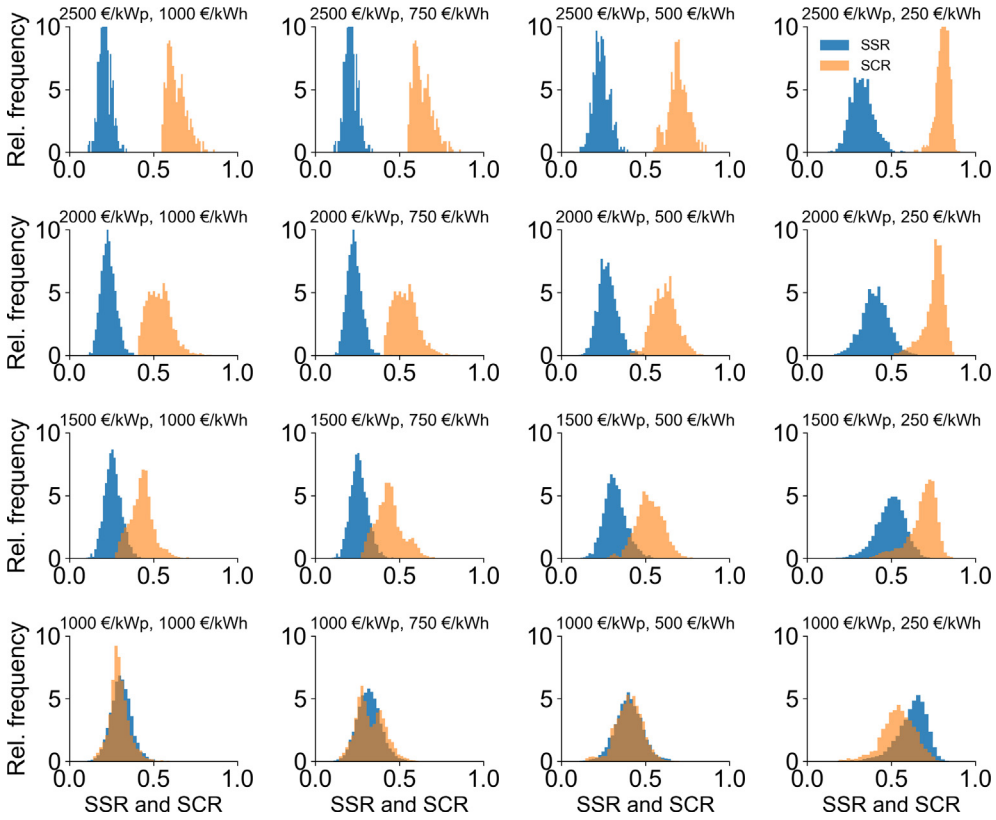


**Fig. C.11.** Histogram of the achieved self-sufficiency ratio (SSR) and self-consumption ratio (SCR) for all cost scenarios.

### C.4. Cross validation and error scores of the predictor

#### C.4.1. Cross validation

It is common practice in supervised machine learning to hold out a part of the available data as a test set and to train the machine learning algorithm on the remaining set, referred to as a training set that is not a subset of the test set. Once trained on the training set, the machine learning model then predicts the output factors of the test set and compares it against the true output factors for the evaluation of error scores. In this article we use 90% of the dataset as the training set and the remaining 10% as the test set. In order to avoid overfitting, the dataset is randomly split 10 times, where 10% of the dataset serves as the test set and the remaining 90% as the training set in each of the 10 folds. This procedure is referred to as 10-fold cross validation and commonly applied in machine learning problems [85].

In addition to the 10-fold cross validation, the load shape and the daily mean demand are estimated if only a fraction (snippet) of the annual time series in the test set is known as input for the machine learning model. Therefore we vary the snippet length in intervals of $L = [1,7,14,30,60,90,160]$ days always measured before December 26th 2009. The training data on the other hand spans from July 19th to December 26th.

All algorithms are trained using the random forest regressor. The accuracy of the random forest regressor depends on the number of estimators (i.e., the number of decision trees that make up the forest). We found that 10 estimators are sufficient to predict the requested output factors. Doubling from 10 to 20 estimators increased the $r^2$ less than 1%.

#### C.4.2. Error scores

See Table C.9.

**Table C.9**
Error and $r^2$ scores of the predictors with variable snippet length $L$ (days mesured before Dec. 26th).

| Snippet length $L$ | NPV (€) | | PV power (kWp) | | Battery size (kWh) | | SSR (%) | | SCR (%) | |
|---|---|---|---|---|---|---|---|---|---|---|
| | MAE | $r^2$ | MAE | $r^2$ | MAE | $r^2$ | MAE | $r^2$ | MAE | $r^2$ |
| 1 | 829 | 0.37 | 0.42 | 0.23 | 0.88 | 0.41 | 5.88 | 0.09 | 6.62 | 0.12 |
| 7 | 649 | 0.58 | 0.35 | 0.5 | 0.84 | 0.53 | 5.22 | 0.27 | 6.34 | 0.18 |
| 14 | 620 | 0.62 | 0.32 | 0.58 | 0.83 | 0.56 | 4.92 | 0.37 | 6.14 | 0.23 |
| 30 | 589 | 0.65 | 0.3 | 0.6 | 0.81 | 0.58 | 4.74 | 0.42 | 6.02 | 0.27 |
| 60 | 559 | 0.69 | 0.28 | 0.64 | 0.81 | 0.59 | 4.57 | 0.46 | 5.93 | 0.28 |
| 90 | 520 | 0.73 | 0.27 | 0.66 | 0.8 | 0.6 | 4.44 | 0.5 | 5.83 | 0.31 |
| 160 | 328 | 0.88 | 0.22 | 0.75 | 0.79 | 0.6 | 4.08 | 0.56 | 5.45 | 0.39 |

## References


[1] European Commission. Energy roadmap 2050. Tech rep; 2012. URL < https://ec.europa.eu/energy/sites/ener/files/../2012_energy_roadmap_2050_en_0.pdf > .

[2] European Commission. PV status report 2016. Tech rep; 2016. URL < http://publications.jrc.ec.europa.eu/repository/bitstream/JRC103426/ldna28159enn.pdf > .

[3] REN21. Renewables 2017 global status report. Tech rep; 2017. URL < http://www.ren21.net/gsr_2017_full_report_en > .

[4] International Energy Agency. Snapshot of global photovoltaic markets 2016. Tech rep; 2017. URL < http://www.iea-pvps.org/?id=266 > .

[5] SolarPower Europe. Global market outlook for solar power 2016–2020. Tech rep; 2016. URL < http://www.solareb2b.it/wp-content/uploads/2016/06/SPE_GMO2016_full_version.pdf > .

[6] US Energy Information Administration. More than half of small-scale photovoltaic generation comes from residential rooftops. Tech rep; 2017. URL < https://www.eia.gov/todayinenergy/detail.php?id=31452 > .

[7] Chatzivasileiadi A, Ampatzi E, Knight I. Characteristics of electrical energy storage technologies and their applications in buildings. Renew Sustain Energy Rev 2013;25:814–30. http://dx.doi.org/10.1016/j.rser.2013.05.023.

[8] Nykvist B, Nilsson M. Rapidly falling costs of battery packs for electric vehicles. Nat Clim Change 2015;5(April):329–32. http://dx.doi.org/10.1038/nclimate2564.

[9] Vieira FM, Moura PS, de Almeida AT. Energy storage system for self-consumption of photovoltaic energy in residential zero energy buildings. Renew Energy 2017;103:308–20. http://dx.doi.org/10.1016/j.renene.2016.11.048.

[10] Linssen J, Stenzel P, Fleer J. Techno-economic analysis of photovoltaic battery systems and the influence of different consumer load profiles. Appl Energy 2017;185:2019–25. http://dx.doi.org/10.1016/J.APENERGY.2015.11.088<https://www.sciencedirect.com/science/article/pii/S030626191501538X>.

[11] Karneyeva Y, Wüstenhagen R. Solar feed-in tariffs in a post-grid parity world: the role of risk, investor diversity and business models. Energy Policy 2017;106(February):445–56. http://dx.doi.org/10.1016/j.enpol.2017.04.005.

[12] Beck T, Kondziella H, Huard G, Bruckner T. Assessing the influence of the temporal resolution of electrical load and PV generation profiles on self-consumption and sizing of PV-battery systems. Appl Energy 2016;173:331–42. http://dx.doi.org/10.1016/j.apenergy.2016.04.050.

[13] Nyholm E, Goop J, Odenberger M, Johnsson F. Solar photovoltaic-battery systems in Swedish households Self-consumption and self-sufficiency. Appl Energy 2016;183:148–59. http://dx.doi.org/10.1016/J.APENERGY.2016.08.172<http://www.sciencedirect.com/science/article/pii/S0306261916312806>.

[14] Luthander R, Widén J, Nilsson D, Palm J. Photovoltaic self-consumption in buildings: a review. Appl Energy 2015;142:80–94. http://dx.doi.org/10.1016/j.apenergy.2014.12.028.

[15] Weniger J, Tjaden T, Quaschning V. Sizing of residential PV battery systems. Energy Proc 2014;46:78–87. http://dx.doi.org/10.1016/j.egypro.2014.01.160<http://www.sciencedirect.com/science/article/pii/S1876610214001763>.

[16] Khalilpour KR, Vassallo A. Technoeconomic parametric analysis of PV-battery systems. Renew Energy 2016;97:757–68. http://dx.doi.org/10.1016/j.renene.2016.06.010.

[17] Kästel P, Gilroy-Scott B. Economics of pooling small local electricity prosumers – LCOE & self-consumption. Renew Sustain Energy Rev 2015;51:718–29. http://dx.doi.org/10.1016/j.rser.2015.06.057.

[18] Munkhammar J, Grahn P, Widén J. Quantifying self-consumption of on-site photovoltaic power generation in households with electric vehicle home charging. Sol Energy 2013;97:208–16. http://dx.doi.org/10.1016/j.solener.2013.08.015.

[19] Christof Bucher. Analysis and simulation of distribution grids with photovoltaics. Phd thesis, ETH Zurich; 2014.

[20] Dumont O, Carmo C, Georges E, Quoilin S, Lemort V. Economic assessment of electric energy storage for load shifting in positive energy building. Int J Energy Environ Eng 2017;8(1):25–35. http://dx.doi.org/10.1007/s40095-016-0224-2.

[21] Colmenar-Santos A, Campíñez-Romero S, Pérez-Molina C, Castro-Gil M. Profitability analysis of grid-connected photovoltaic facilities for household electricity self-sufficiency. Energy Policy 2012;51:749–64. http://dx.doi.org/10.1016/j.enpol.2012.09.023.

[22] Cerino Abdin G, Noussan M. Electricity storage compared to net metering in residential PV applications. J Cleaner Prod 2018;176:175–86. http://dx.doi.org/10.1016/J.JCLEPRO.2017.12.132<http://www.sciencedirect.com/science/article/pii/S0959652617330913>.

[23] Camilo FM, Castro R, Almeida M, Pires VF. Economic assessment of residential PV systems with self-consumption and storage in Portugal. Sol Energy 2017;150:353–62. http://dx.doi.org/10.1016/J.SOLENER.2017.04.062<http://www.sciencedirect.com/science/article/pii/S0038092X17303675>.

[24] Quoilin S, Kavvadias K, Mercier A, Pappone I, Zucker A. Quantifying self-consumption linked to solar home battery systems: statistical analysis and economic assessment. Appl Energy 2016;182:58–67. http://dx.doi.org/10.1016/J.APENERGY.2016.08.077<http://www.sciencedirect.com/science/article/pii/S0306261916311643>.

[25] Karakaya E, Hidalgo A, Nuur C. Motivators for adoption of photovoltaic systems at grid parity: a case study from southern Germany. Renew Sustain Energy Rev 2015;43:1090–8.

[26] Mulder G, Six D, Claessens B, Broes T, Omar N, Mierlo JV. The dimensioning of PV-battery systems depending on the incentive and selling price conditions. Appl Energy 2013;111:1126–35. http://dx.doi.org/10.1016/j.apenergy.2013.03.059<http://www.sciencedirect.com/science/article/pii/S0306261913002559>.

[27] Bertsch V, Geldermann J, Lühn T. What drives the profitability of household PV investments, self-consumption and self-sufficiency? Appl Energy 2017;204:1–15. http://dx.doi.org/10.1016/j.apenergy.2017.06.055. Available from: arXiv:suresh govindarajan <http://www.sciencedirect.com/science/article/pii/S0306261917308073>.

[28] Graebig M, Erdmann G, Röder S. Assessment of residential battery systems (RBS): profitability, perceived value proposition, and potential business models. In: 37th IAEE international conference, vol. 25; 2014. p. 1–15.

[29] Zhang C, Wu J, Cheng M, Zhou Y, Long C. A bidding system for peer-to-peer energy trading in a grid-connected microgrid. Energy Proc 2016;103:147–52. http://dx.doi.org/10.1016/j.egypro.2016.11.264<http://linkinghub.elsevier.com/retrieve/pii/S1876610216314746>.

[30] de Oliveira e Silva G, Hendrick P. Photovoltaic self-sufficiency of Belgian households using lithium-ion batteries, and its impact on the grid. Appl Energy 2017;195:786–99. http://dx.doi.org/10.1016/j.apenergy.2017.03.112.

[31] Luthander R, Widén J, Nilsson D, Palm J. Photovoltaic self-consumption in buildings: a review. Appl Energy 2015;142:80–94. http://dx.doi.org/10.1016/j.apenergy.2014.12.028.

[32] Parra D, Patel MK. Effect of tariffs on the performance and economic benefits of PV-coupled battery systems. Appl Energy 2016;164:175–87. http://dx.doi.org/10.1016/j.apenergy.2015.11.037<http://www.sciencedirect.com/science/article/pii/S0306261915014877>.

[33] Merei G, Moshövel J, Magnor D, Sauer DU. Optimization of self-consumption and techno-economic analysis of PV-battery systems in commercial applications. Appl Energy 2016;168:171–8. http://dx.doi.org/10.1016/j.apenergy.2016.01.083<http://www.sciencedirect.com/science/article/pii/S0306261916300708>.

[34] Johann A, Madlener R. Profitability of energy storage for raising self-consumption of solar power: analysis of different household types in Germany. Energy Proc 2014;61:2206–10.

[35] Tjaden T, Weniger J, Bergner J, Schnorr F, Quaschning V. Einfluss des standorts und des nutzerverhaltens auf die energetische bewertung von pv-speichersystemen. In: 29. Symposium Photovoltaische Solarenergie; 2014.

[36] Zhang Y, Campana PE, Lundblad A, Yan J. Comparative study of hydrogen storage and battery storage in grid connected photovoltaic system: storage sizing and rule-based operation. Appl Energy 2017;201:397–411. http://dx.doi.org/10.1016/J.APENERGY.2017.03.123<https://www.sciencedirect.com/science/article/pii/S0306261917303690>.

[37] Kaschub T, Jochem P, Fichtner W. Solar energy storage in German households: profitability, load changes and flexibility. Energy Policy 2016;98:520–32. http://dx.doi.org/10.1016/J.ENPOL.2016.09.017<https://www.sciencedirect.com/science/article/pii/S0301421516304815?via%3Dihub>.

[38] Mulder G, Six D, Claessens B, Broes T, Omar N, Mierlo JV. The dimensioning of PV-battery systems depending on the incentive and selling price conditions. Appl Energy 2013;111:1126–35. http://dx.doi.org/10.1016/J.APENERGY.2013.03.059<http://www.sciencedirect.com/science/article/pii/S0306261913002559>.

[39] Hoppmann J, Volland J, Schmidt TS, Hoffmann VH. The economic viability of battery storage for residential solar photovoltaic systems – a review and a simulation model 2014. http://dx.doi.org/10.1016/j.rser.2014.07.068.

[40] Bortolini M, Gamberi M, Graziani A. Technical and economic design of photovoltaic and battery energy storage system. Energy Convers Manage 2014;86:81–92. http://dx.doi.org/10.1016/j.enconman.2014.04.089 < http://linkinghub.elsevier.com/retrieve/pii/S0196890414004014 > .

[41] Meunier J, Knittel D, Collet P, Sturtzer G, Carpentier C, Rocchia G, et al. Sizing of a photovoltaic system with battery storage: influence of the load profile. In: CISBAT 2015; September 9–11, 2015. p. 711–6.

[42] Khalilpour R, Vassallo A. Leaving the grid: an ambition or a real choice? Energy Policy. http://dx.doi.org/10.1016/j.enpol.2015.03.005.

[43] Schopfer S, Tiefenbeck V, Staake T. Untersuchung des Selbstversorgungsgrades und der Wirtschaftlichkeit von PV-Batterie Systemen anhand eines grossen Smart-Meter Datensatzes. In: 14. Symposium Energieinnovation; 2016.

[44] Linssen J, Stenzel P, Fleer J. Techno-economic analysis of photovoltaic battery systems and the influence of different consumer load profiles. Appl Energy. http://dx.doi.org/10.1016/j.apenergy.2015.11.088.

[45] Swiss Federal Office of Energy). Schweizerische Statistik der erneuerbaren Energien. Ausgabe 2015. Tech rep; 2016. URL < http://www.bfe.admin.ch/php/modules/publikationen/stream.php?extlang=de&name=de_818961010.pdf > .

[46] Swiss Federal Officie of Energy. Schweizerische Elektrizitätsstatistik 2016. Tech rep; 2016. URL < http://www.bfe.admin.ch/themen/00526/00541/00542/00630/index.html?lang=en&dossier_id=00765 > .

[47] Bundesamt für Energie. Förderung der Photovoltaik Faktenblatt. Tech rep; 2017. URL < http://www.bfe.admin.ch/themen/00612/05410/06149/index.html?lang=de&dossier_id=06150 > .

[48] Verband unabhängiger Energieerzeuger. Overview of Swiss renumeration tariffs for PV systems [accessed 27th of March 2018]. URL < http://www.vese.ch/pvtarif/ > .

[49] CER. CER dataset. URL < http://www.ucd.ie/issda/data/commissionforenergyregulationcer/ > .

[50] EurObserv'ER. Photovoltaic barometer. Tech rep; 2017. URL < https://www.eurobserv-er.org/photovoltaic-barometer-2017/ > .

[51] Parra D, Gillott M, Norman SA, Walker GS. Optimum community energy storage system for PV energy time-shift. Appl Energy 2015;137:576–87. http://dx.doi.org/10.1016/j.apenergy.2014.08.060 < http://www.sciencedirect.com/science/article/pii/S030626191400871X > .

[52] WeatherAnalaytics. Weather analytics. URL < http://www.weatheranalytics.com > .

[53] Paulescu M, Paulescu E, Gravila P, Badescu V. Weather modeling and forecasting of PV systems operation. Springer; 2013. http://dx.doi.org/10.1007/978-1-4471-4649-0.

[54] Michael A, Konersmann L, Wanner A, Suter M. PV-Preisumfrage 2015. Tech rep. Energiezukunft Schweiz; 2016.

[55] Li R, Shaddick G, Yan H, Li F. Sample size determination of photovoltaic by assessing regional variability. In: CIRED workshop 2014, Rome, Italy; 2014. p. 1–5.

[56] GoGreenSolar.com. SolarWorld panels—260 Watt mono black solar panel—buy SolarWorld PV solar panels. URL < https://www.gogreensolar.com/products/solarworld-sw-260-mono-black-260-watt-solar-panel > .

[57] SolaxPower. SolaxPower X Product Sheet.

[58] Speichermonitoring.de. Batterietechnologien und Preise. URL < http://www.speichermonitoring.de/ueber-pv-speicher/batterietechnologien.html > .

[59] Fraunhofer ISE. Aktuelle Fakten zur Photovoltaik in Deutschland (last amended on 21st of February 2018). Tech Rep. 0; Fraunhofer 2018.

[60] Swiss Federal Office of Energy. Strompreisentwicklung in der Schweiz. Tech rep; 2011.

[61] EWZ. EWZ Tarifs; 2016. URL < https://www.ewz.ch/content/dam/ewz/services/dokumentencenter/energie-beziehen/dokumente/gruener-strom-fuer-mein-zuhause/stromtarif-2016-zh-private.pdf > .

[62] Swiss Administration. SR 730.0 Energiegesetz vom 30. September 2016 (EnG) Stand 1.Januar 2018; 2018. URL < https://www.admin.ch/opc/de/classified-compilation/20121295/index.html > .

[63] SFOE. Einmalvergütung und Eigenverbrauch: Informationen für Projektanten von kleinen Photovoltaik-Anlagen. Tech rep. Swiss Federal Office of Energy (SFOE); 2016.

[64] Dehler J, Keles D, Telsnig T, Fleischer B, Baumann M, Fraboulet D, et al. Self-consumption of electricity from renewable sources. Europe's energy transition – insights for policy making Elsevier; 2017. p. 225–36. http://dx.doi.org/10.1016/B978-0-12-809806-6.00027-4 < http://linkinghub.elsevier.com/retrieve/pii/B9780128098066000274 > .

[65] C.A.-R.M. und Energienetzwerk. Marktübersicht Batteriespeicher.

[66] Truong C, Naumann M, Karl R, Müller M, Jossen A, Hesse H. Economics of residential photovoltaic battery systems in Germany: the case of Tesla's powerwall. Batteries 2016;2(2):14. http://dx.doi.org/10.3390/batteries2020014 < http://www.mdpi.com/2313-0105/2/2/14 > .

[67] Wagner Solar. Supplier price list provided on request in Feb. 2018; 2018. URL < http://www.wagner-solar.com/ > .

[68] IEA. Technology roadmap: solar photovoltaic energy. Tech rep. IEA; 2014. http://dx.doi.org/10.1007/SpringerReference_7300. URL < http://www.iea.org/publications/freepublications/publication/TechnologyRoadmapSolarPhotovoltaicEnergy_2014edition.pdf > .

[69] EPIA. Global market outook for photovoltaics 2014–2018. Tech rep. European Photovoltaic Industry Association; 2014.

[70] Fraunhofer ISE, Wirth H. Aktuelle Fakten zur Photovoltaik in Deutschland (amended on 21st of February 2018) . Tech rep; 2018. URL < https://www.ise.fraunhofer.de/content/dam/ise/de/documents/publications/studies/aktuelle-fakten-zur-photovoltaik-in-deutschland.pdf > .

[71] Bertsch V, Geldermann J, Lühn T. What drives the profitability of household PV investments, self-consumption and self-sufficiency? Appl Energy 2017;204:1–15. http://dx.doi.org/10.1016/J.APENERGY.2017.06.055 < https://www.sciencedirect.com/science/article/pii/S0306261917308073 > .

[72] Breiman L. Random forests. Mach Learn 2001;45(1):5–32. http://dx.doi.org/10.1023/A:1010933404324.

[73] Graziano M, Gillingham K. Spatial patterns of solar photovoltaic system adoption: the influence of neighbors and the built environment. J Econ Geogr 2015;15(4):815–39. http://dx.doi.org/10.1093/jeg/lbu036. Available from: arXiv:/oup/backfile/content_public/journal/joeg/15/4/10.1093_jeg_lbu036/2/lbu036.pdf.

[74] Griskevicius V, Tybur JM, Van den Bergh B. Going green to be seen: status, reputation, and conspicuous conservation. J Person Soc Psychol 2010;98(3):392–404. http://dx.doi.org/10.1037/a0017346. < http://www.ncbi.nlm.nih.gov/pubmed/20175620 > .

[75] Masa-Bote D, Castillo-Cagigal M, Matallanas E, Caamao-Martn E, Gutirrez A, Monasterio-Hueln F, et al. Improving photovoltaics grid integration through short time forecasting and self-consumption. Appl Energy 2014;125:103–13. http://dx.doi.org/10.1016/j.apenergy.2014.03.045 < http://www.sciencedirect.com/science/article/pii/S0306261914002761 > .

[76] Staffell I, Rustomji M. Maximising the value of electricity storage. J Energy Storage 2016;8:212–25. http://dx.doi.org/10.1016/j.est.2016.08.010 < http://www.sciencedirect.com/science/article/pii/S2352152X1630113X > .

[77] Schopfer S, Tiefenbeck V, Fleisch E, Staake T. Effect of tariff arbitrage on photovoltaic battery economics using predictive control 2016.

[78] Jin M, Feng W, Liu P, Marnay C, Spanos C. MOD-DR: microgrid optimal dispatch with demand response. Appl Energy 2017;187:758–76.

[79] Hussein AA-H, Batarseh I. An overview of generic battery models. 2011 IEEE power and energy society general meeting IEEE; 2011. p. 1–6. http://dx.doi.org/10.1109/PES.2011.6039674 < http://ieeexplore.ieee.org/document/6039674/ > .

[80] Newman J, Tiedemann W. Porous-electrode theory with battery applications. AIChE J 1975;21(1):25–41. http://dx.doi.org/10.1002/aic.690210103.

[81] Stephan A, Battke B, Beuse MD, Clausdeinken JH, Schmidt TS. Limiting the public cost of stationary battery deployment by combining applications. Nat Energy 2016;1(June):16079. http://dx.doi.org/10.1038/nenergy.2016.79 < http://www.nature.com/articles/nenergy201679 > .

[82] Vayá MG, Andersson G. Optimal bidding of plug-in electric vehicle aggregator in day-ahead and regulation markets Marina González Vayá ∗ and Göran Andersson. Int J Electr Hybrid Veh 2015;7(3). http://dx.doi.org/10.1504/IJEHV.2015.071642.

[83] Timeanddate.com. Sunrise and sunset times in Ireland; July 2018. URL < https://www.timeanddate.com/sun/@2963597?month=7&year=2018 > .

[84] Holiday-Weather.com. Weather and temperature averages for Dublin, Ireland. URL < http://www.holiday-weather.com/dublin/averages/ > .

[85] James G, Witten D, Hastie T, Tibshirani R. An introduction to statistical learning; 2013. Available from: arXiv:1011.1669v3. http://dx.doi.org/10.1007/978-1-4614-7138-7.